An elemental and 87Sr/86Sr isotopic restitution of contaminated pore waters from sandy sediments of the Peciko gas field (Mahakam Delta, Indonesia)

Norbert Clauer

An elemental and $^{87}Sr/^{86}Sr$ isotopic restitution of contaminated pore waters from sandy sediments of the Peciko gas field (Mahakam Delta, Indonesia)

Norbert Clauer[(1)]

[(1)] Institut de Physique du Globe de Strasbourg, Université de Strasbourg (UdS/CNRS), 1 Rue Blessig, 67084 Strasbourg, France

corresponding author: Dr. Norbert Clauer, Institut de Physique du Globe de Strasbourg, Université de Strasbourg (UdS/CNRS), 1 Rue Blessig, 67084-Strasbourg, France ; e-mail: nclauer@unistra.fr

keywords: restored pore waters; H_2O and dilute HCl leachates; $^{87}Sr/^{86}Sr$ ratios; major, trace and rare-earth elemental contents; Peciko gas field; Mahakam Delta (Indonesia)

Abstract

Pore waters of hydrocarbon-bearing sand layers from gigantic Peciko gas reservoir located to the South of the Mahakam Delta in Indonesia were reconstructed and studied by applying the restored pore-water technique. The method is based on the Sr isotopic compositions of rock chips leached with de-ionized water aided, here, by the associated contents of major, metal and rare-earth elements (REEs). The soluble minerals were also leached with dilute hydrochloric acid and analyzed for their Sr isotopic compositions.

The main founding is that many of the recovered H_2O leachates were most probably contaminated during coring, which induced abnormally high metal and REE contents. The leachates considered free of pollution yield $^{87}Sr/^{86}Sr$ ratios that increase progressively with depth, which suggests a recent supply of surface waters to the upper pore waters. It seems also that only a few sedimentary horizons are interconnected at intermediate depths. Furthermore, the minerals dissolved by dilute HCl yield quite systematically lower $^{87}Sr/^{86}Sr$ ratios than the

associated pore waters, which suggests a crystallization earlier than the recent flushing of the upper sediments by surface-type waters.

1. Introduction

The chemical evolution of oil-field waters and their migration paths have often been reconstructed successfully on the basis of their chemical and stable isotope data (e.g., Sulin, 1947; De Sitter, 1947; Degens et al., 1964; White, 1965; Clayton et al., 1966; Rittenhouse, 1967; Hitchon et al., 1971; Kharaka et al., 1973; Kharaka and Berry, 1974; Collins, 1975; Carpenter, 1978). As fluid-rock interactions play key roles in the compositional evolution of these waters, a reconstruction of their interactions requires varied chemical and isotopic information. For instance, such studies ignored largely the potential benefits that may come from Sr isotopic investigations until Chaudhuri's (1978) publication, which was confirmed by many further studies (e.g., Sunwall and Pushkar, 1979; Starinsky et al., 1983; Chaudhuri et al., 1983; Stueber et al., 1984; Chaudhuri et al., 1987; Furlan et al., 1995). These studies not only provided valuable clues to the understanding of the chemical evolution of oil-field waters, but also improved the comprehension of the diagenetic history of their host rocks.

While long-distance migrations of pore waters through various rock types of any sedimentary basin often obscure the reconstruction of their geochemical evolution, their study may provide valid information within a finite space and during a limited time in a basin. In this context, it appeared of interest to test the Sr isotope compositions of restored formation waters following the "Residue Salt Analysis" concept of Stolum et al. (1993) complemented by elemental analyses of the leachates, and by Sr isotopic data obtained on the soluble minerals of the studied rocks by interaction with dilute hydrochloric acid. The purpose was to pursue testing that isotopic technique by identifying connections between producing units of larger hydrocarbon reservoirs. More precisely, the isotopic technique was applied here, together with elemental analyses of the H_2O leachates on hydrocarbon-bearing sand units of the gigantic Peciko reservoir to the South of the Mahakam Delta in Indonesia.

2. Geological and hydrodynamic background

The Mahakam delta is located on the eastern side of Borneo Island in Indonesia (Fig. 1). Active since the Pliocene, the river deposited more than 10,000 m of interlayered lithic

sandstone and shale units into the delta (Duval et al., 1992). The collecting basin corresponds to the limited drainage surface of the nearby island that does not host any Sr-rich carbonate-type rocks. This lack of outcropping carbonates is of some importance in the further discussion, because it means that the river waters were not enriched in overwhelming Sr contents that could have imprinted preferentially the $^{87}Sr/^{86}Sr$ ratio of the local surface waters from deposited sediments. The surface drained by the Mahakam River is only of about 75,000 km^2, which means that the chemical signatures of the present-day pore waters are most likely not obscured by multiple and extensive interactions with various types of rocks during a long-distance migration, as is the case for pore waters from large sedimentary basins of North America (e.g., Chaudhuri et al., 1987; Banner et al., 1989). The gentle Miocene deformation of the Mahakam sedimentary sequence into successive anticlines was followed by some late reactivations (Letouzey et al., 1990). Consequently, the oil and gas fields of the Mahakam Delta basin relate to anticline traps oriented parallel to the coastline with the Peciko-Handil-Tambora-Badak axis being the closest to the shore (Fig. 1).

Onshore exploration of hydrocarbons in the area started before the turn of the last century. A system of hydrodynamic brine circulations flowing in opposite directions was described (Grosjean et al., 1994) due to an onshore uplift allowing meteoric waters to invade permeable intervals of the stratigraphic section, mostly at the faulted edges of the deltaic offshore system. Also, a deeper and slower, but more extensive, circulation of brines was driven by overpressures found in distal shales (Burrus et al., 1992). The available chemical and isotopic data of formation waters from proximal (Tambora and Handil) and distal (Attaka and Bekapai) oil fields provided more information about the recent to present-day mass transfers (Furlan et al., 1995). For instance, the Ca and Sr contents decrease in the formation waters, whereas the Sr/Ca ratio suggests a combined precipitation of albite and dissolution of K-feldspar, while the associated decrease of the released K in the running waters was consumed by an on-going illitization. The variations in the $^{87}Sr/^{86}Sr$ ratio of the waters were related to the dissolution of these K-feldspar minerals.

The influence of down-dip hydrodynamic circulations on the lateral sealing of the local stratigraphic traps was explained by a system consisting of meteoric waters driven by gravity (e.g., Stones and Hoeger, 1973). Drilling of the Peciko-1 well in the early 1990s into the northwestern area of the field was somehow determining as pressure-depth plots could be documented in the upper sections that showed aligned gas-pressure curves. These curves revealed that many large reservoirs were detected, each consisting of multiple-metric sand bodies. Thicker shale inter-beds could also be correlated regionally on the basis of

intersecting sand bodies that resulted from flooding events in the deltaic environment with seals as useful tools for the pressure profiles.

Twenty-three core samples were collected for the present study along the Peciko-3 and Peciko-8 wells drilled into the northwestern Peciko gas field (Fig. 1). Nine of these samples belong to the upper zone of the P3 well between the markers MF7 and MF75 from 2,730 to 2,780 m depth (Fig. 2). Seven more samples were collected in the upper intermediate P3-ZI zone between the markers MF8 and FS85.1 from 3,110 to 3,180 m. Three more samples are from lower intermediate zone P3-ZII between the markers FS85.4 and FS85.6 at about 3,380 m, while the four last samples belong to the deeper P3-ZP zone below the marker MF9, at 3,510 to 3,560 m. Nine additional samples were collected in the nearby Peciko-8 well; two of them being parts of the upper zone at 2932.6 and 2959.4 m, two others belonging to the intermediate zone at 3,320.4 and 3,322.4 m, while the last five range between 3,506 and 3,538 m.

3. Analytical procedure

The analytical procedure is based on the concept of Stolum et al. (1993) called "Residue Salt Analysis". Those authors demonstrated that hydrocarbon-bearing reservoirs from a North Sea reservoir communicate or not on the basis of Sr isotopic data of deionized-water leachates of the reservoir rocks. If two reservoirs were or still are connected, the $^{87}Sr/^{86}Sr$ ratio of the rock leachates should overlap as they may be considered to be representative of seeping formation brines. Conversely, in the case of non-communicating reservoirs, the same isotopic ratios should not overlap. The cores studied here were first hand-cleaned by removing the external centimeter-thick layer potentially contaminated by drilling mud. Then, they were gently reduced into centimeter-large chips by hammer crushing, and the rock chips were subjected to a one-hour interaction in a satellite rotating equipment with deionized water at a 2 to 1 water/rock weight ratio. Afterwards, the leachates and residues were centrifuged at about 4,500 rpm during 1 hr, the leachates being collected for analysis and the residues for further leaching. This further leaching was similar to the previous one, except for the reagent, the de-ionized water being replaced by ultra-pure HCl diluted to 1M at an acid-rock weight ratio set at a 1 to 1 for a 15-mn interaction.

The leachates were dried in Teflon© beakers and the residues dissolved in HNO_3 acid before analysis. The contents of the major, trace and rare-earth elements (REEs) were analyzed on an Inductively Coupled Plasma-Atomic Emission Spectrometer (ICP-AES) for

the major elements and on an Inductively Coupled Plasma-Mass Spectrometer (ICP-MS) for the trace and REEs, following Samuel et al.'s (1985) procedure. Reproducibility tests were made routinely by a systematic analysis of the international BE-N and GL-O standards that give a reproducibility of the equipment at a 2.5% uncertainty for the major elements that doubles at 5% for the trace elements, and again at 10% for the REEs.

The Sr isotopic data were determined on a mass spectrometer with a multi-collector. Strontium of the leachates was separated and purified using a chemical procedure similar to that reported by Schaltegger et al. (1994) and loaded on Ti-filaments for analysis. The $^{87}Sr/^{86}Sr$ value of the NBS 987 standard was 0.710257 ± 0.000015 (2σmean external) for 4 independent analyses during the study. A systematic internal uncertainty of $2\sigma/\sqrt{N}$ is given for each measured $^{87}Sr/^{86}Sr$ ratio on the basis of a hundred measured ratios (Table 1).

4. Results

4.1. The $^{87}Sr/^{86}Sr$ ratio of the H_2O and HCl leachates

The $^{87}Sr/^{86}Sr$ ratio of the H_2O leachates increases with depth: the upper scatter ranges from 0.70852 to 0.70898 at 2,700-2,800 m depth and increases to 0.70987 at 3,500 m (Table 1). If combined with the Rb/Sr ratio, which might have an impact due to the production of ^{87}Sr due to the decay of ^{87}Rb relative to time, it might result from mixtures with various ratios. The data points fit two lines in a diagram with steep slopes that include most data points with intercepts with the $^{87}Sr/^{86}Sr$ abscissa at about 0.7084. Five more dispersed data points with higher Rb/Sr ratios are also scattered to the lower right side of the diagram (Fig. 3A). The H_2O leachates of the Peciko-8 samples display a similar pattern for the $^{87}Sr/^{86}Sr$ ratio relative to the Rb/Sr ratio (Fig. 3B). All their data, except one, fit again two lines with steep slopes that intercept again the abscissa at about 0.7084. Interestingly, the data points that plot outside the two lines in the two drillings belong to the uppermost samples.

The $^{87}Sr/^{86}Sr$ ratios of the HCl leachates display a similar spread relative to depth than those of the corresponding H_2O leachates, in both drill wells (Fig. 4). The ratios increase progressively with depth, being more scattered in the Peciko-8 drilling well. They are also systematically lower than those of the corresponding H_2O leachates except for the sample at 2778.7 m depth in the Peciko-3 well (Table 1; Fig. 5A). In fact, the overall differences among the $^{87}Sr/^{86}Sr$ ratios of the two types of leachates tange from 2.9×10^{-5} to 98.1×10^{-5} (Fig. 5B). The largest differences ($> 50.0\times10^{-5}$) were obtained mostly in the leachates of the deeper samples from the two wells.

A comparison of the $^{87}Sr/^{86}Sr$ ratios from the successive H_2O and HCl leachates of the same rock samples shows that the ratios of the formers are higher than those of the latters, except the already mentioned sample (Fig. 5A). This overall behavior is confirmed by the data of the leachates from second drilling well (Fig. 5B). The two diagrams show also that the difference among the $^{87}Sr/^{86}Sr$ ratios of the two types of leachates is somewhat stratified, the larger differences being for the deeper H_2O leachates relative to those with HCl. However, no clearly organized stratification can be observed within each collection depth.

4.2. The major and trace elemental contents of the H_2O leachates

A preliminary comment about the changing contents of the major and trace elements from H_2O leachates is probably appropriate to avoid any confusion. The released contents were made, here, on "restored" waters and not strictly on "pore" waters. The purpose was not to discuss the concentrations of formation waters taken at different depths, but to compare extraction contents of "reconstructed" fluids. The goal was, therefore, not to calculate concentrations that are also dependent on the relative porosity of the host rocks, but to follow an analytical dispersion of the contents relative to depth. However, it can certainly be agreed that the porosity of the deeper samples is lower than that of less deeply collected samples.

In turn, the contents in major elements of the restored formation waters obtained here by leaching the rock samples from the two wells with de-ionized water show a general tendency to decrease with depth (Fig. 6). The elemental contents of the same waters from the second drilling well fit the range of those from first drilling, except for a very high Fe_2O_3 content in its deeper section. Also to be noticed are the generally low Rb and Fe contents (Table 2; Fig. 7), the contents of elements such as Al, Rb and Sr that appear to be quite widely dispersed at the intermediate depth range of 3,100-3,200 m.

To overcome the missing porosity values of the sediments, some major and trace elements were also compared relative to their sampling depth in the sediments. The spread of the Si/Al ratio becomes wider towards depth, which is mainly due to a downward decrease of the Al contents (Table 2; Fig. 7). On the other hand, the Si/Fe ratio decreases with depth increase, except for one value. Widely scattered near the surface, the Ca/Sr decreases also with depth, except again, one deeper value. Chosen because of potential interactions between formation waters and carbonates, this Ca/Sr ratio is the widest dispersed at the upper collection depths (Table 1), while decreasing significantly at the two intermediate depths and increasing again in the deepest. These changes appear to be mostly related to the changes in the Sr contents. The Rb/Sr ratio that might impact the $^{87}Sr/^{86}Sr$ ratio of the formation waters

due to the leaching of radiogenic ^{87}Sr released from alkali-rich soluble minerals, is also decreasing with depth, except one intermediate sample, which can be related to a Sr increase in the deeper extracts (Fig. 7). It shows a clear difference between the restored waters of the two drillings. The ratios of the H_2O leachates from Peciko-3 well are quite higher than those of the sister drilling, especially in the deepest collection range.

The contents of metallic elements (Cr, Co, Ni, Cu, Zn, Br, Ba, Cs and Sn) from H_2O leachates were also determined (Table 3). While those of Cs and Sn remain systematically low, which testifies for reliable data, those of the other metals are extremely varied with very high values, for instance from 2.3 to 637 ng/g for Cr or from 1.1 to 923 ng/g for Ni in leachates from Peciko-3 well (Fig. 8). In fact, Co, Ni, Cu and Zn vary together within very wide ranges in three leachates of this Peciko-3 drill hole. The Br contents are also very variable between 13.7 and 661 ng/g in the leachates of the same well. The uppermost samples are systematically widely spread with very high contents. These large scatters for the H_2O leachates, and especially the high contents of similar metals for the reconstructed pore waters of quite homogeneous host rocks, are somehow surprising and even suspicious.

4.3. The contents and distribution of the rare-earth elements in the H_2O leachates

The total REE concentrations also range widely from 0.46 to 359 ng/g for the H_2O leachates when the patterns are complete that is to say without any of the REEs below detection limit (Table 4). As for the metal contents, the higher contents are somewhat intriguing: two total amounts are beyond 340 ng/g and two others are at 117-144 ng/g. Three of those were obtained on leachates from upper section of the Peciko-3 well and one from deeper part of the Peciko-8 well. In fact, such high REE contents are not expected in H_2O leachates, as natural waters are known to yield low to very low REE concentrations due to the low solubility of the REEs and their tendency to adsorb preferentially onto particle surfaces (e.g., Taylor and McLennan, 1985).

The total REE contents above 100 ng/g give smooth patterns relative to the Post Archean Australian Shales (PAAS) taken here as reference, with a regular increase from La until Eu, an almost regular flat plateau for the successive Eu, Gd and Tb and a final, smooth decrease until Lu (Fig. 9, upper row). This configuration is still obtained for leachates with contents up to 27-ng/g with, however, a more irregular distribution for the heavy REEs (HREEs; Fig. 9, middle row). Below total contents of 4 ng/g, the patterns become much more irregular with higher Eu values relative to the PAAS that are equivalent to those of Gd (Fig. 9, middle row). In the REEs patterns of H_2O leachates with total values below 1 ng/g, the Eu

content is systematically the lowest of the surrounding REEs, that of Tb becoming the highest (Fig. 9, lower row). Of course, such low concentrations are somehow biased by high uncertainties beyond the usual +/-10% uncertainty given by the repetitive analysis of the international standards, which probably contributes, at least partly, to the observed irregular shapes.

If discarding all REE contents above a total of 27.1 ng/g, the contents range from 0.34 to 10.3 ng/g for the patterns with no more than one element below the detection limit (Table 4). Based on this adjustment, the total contents decrease relative to collection depth with systematic contents below 1 ng/g in the H_2O leachates of the deeper samples from both wells. However, for analytical reasons and consequently because of the large uncertainties in such low contents, only the REE spectra amounting between 10 and 1 ng/g were evaluated further. Also of interest, the La/Yb ratio varies widely from 0.08 to 3.30, with five values that could not be measured because the contents of either La and/or Yb were below the detection limit. In the detail, high contents of REEs and of metals were found together in two samples of the Peciko-3 well at 2,768 and 2,779 m depth, as well as in two samples of the Peciko-8 well at 2,932 and 3,516 m depth. These large scatters with abnormal high values, together with those of the metals, suggest clearly a contamination to be identified.

5. Discussion

Among the preliminary observations are the $^{87}Sr/^{86}Sr$ ratios of the restored formation waters increasing with depth, whereas their elemental contents decrease correlatively. The Sr isotopic ratios of the HCl leachates from the same samples are also systematically lower than those of the corresponding H_2O leachates, including an increase with depth. And, importantly, the distribution patterns of the REEs relative to the PAAS reference, as well as the high metal contents, seem to depend more on their amounts than on the burial depth.

5.1. The meaning of the elemental and Sr isotopic data of the H_2O leachates

The increasing $^{87}Sr/^{86}Sr$ ratios of the H_2O leachates downward the sedimentary sequence, with a decrease of the elemental contents, (Fig. 4 and 6) suggests an overall chemical heterogeneity of the leachates, as well as a kind of stratification from upper to deeper sampling depth. This combination is confirmed by the data of the H_2O leachates of the samples from the second well. The individual data of the successive collection strata also show that no identical to close $^{87}Sr/^{86}Sr$ values are obtained on most successive restored water

samples. This observation is confirmed by the REE data that are highly variable in their contents for each collection leyer, as well as by their distribution patterns relative to the PAAS reference.

For instance, the widely spread REE and metal contents of the restored pore waters need an explanation. Spontaneously, such data may be due to a contamination, either natural or anthropogenic, due to an addition of natural waters from outside the field and/or, probably, resulting from a human activity. If one agrees that this contamination is highest with REE contents at about 350 ng/g in the leachates and that it is vanishing at about 5 ng/g, the range can be compared to the corresponding major and trace elements and to the $^{87}Sr/^{86}Sr$ ratios. Those leachates with such high REE contents yield also high Ca and Sr contents above 100 and 200 ng/g, respectively (Table 5). In turn a solid indicator of the contamination seems to be the Ca/Sr ratio that is beyond about 0.5 in most samples. If the same criteria are applied to the $^{87}Sr/^{86}Sr$ ratio of the leachates, those contaminated have a tendency to occur rather on the high side of the elemental data, especially at the upper collection level (Fig. 6; the gray dots). These low $^{87}Sr/^{86}Sr$ ratios relative to contemporaneous pore-water layers could then be due, based on the REE data, to the addition of present-day water and/or drilling fluids that could have been used during the exploration drillings.

Combined with the Rb/Sr ratio, the $^{87}Sr/^{86}Sr$ ratios of the H_2O leachates from very upper sampling depths plot away from common evolution lines, representing in turn a further argument in favor of a recent to very recent external supply (Fig. 5A). Indeed, all leachates with data points outside the two lines could result, at least partly, from recent addition(s) of external natural waters. About the potential origin of these waters, McArthur et al. (2001) showed that the $^{87}Sr/^{86}Sr$ ratio of the ocean water increased after the Oxfordian, albeit with small reversals, to reach a today's high of 0.709175 that is far beyond the $^{87}Sr/^{86}Sr$ ratio of the restored waters determined here. It can then be stated that the water used during the injection of any kind of product into the drill holes was not ocean water, but rather that of the Mahakam River in the delta.

In summary and beyond the analytical heterogeneity due to a probable pollution by the drilling of the wells, the elemental and Sr isotopic data show that there is no straight continuity in most successive collected samples of the two wells studied here. There are almost never elemental and Sr isotopic continuities in successively analyzed H_2O leachates, whatever the burial depth of the host samples. About the drilling pollutant, it obviously increases the REE, Ca, Sr and metal contents and decreases the $^{87}Sr/^{86}Sr$ ratio of the leachates.

305 5.2. The meaning of the $^{87}Sr/^{86}Sr$ ratio of the H_2O and the HCl leachates

306 The differences among the $^{87}Sr/^{86}Sr$ ratio of the H_2O and the HCl leachates are widely
307 scattered from $2.9x10^{-5}$ to $98.1x10^{-5}$ in favor of the H_2O leachates, the larger differences
308 occurring at depth. Before discussing a possible geochemical continuity among the upper and
309 deeper restored waters, two preliminary hypotheses can be launched beyond the already
310 evidenced contamination: (1) either the overall increase of the $^{87}Sr/^{86}Sr$ ratio relative to depth
311 is due to a variable incorporation of ^{87}Sr into the pore fluids resulting from interactions with
312 host minerals fueled by an increasing diagenetic action monitored by a general increase of the
313 burial temperature, or (2) the deeper fluids are significantly "older" than the upper ones with
314 probable impermeable units in between, an argument that is supported by the elemental and
315 Sr isotopic differences even in the same sequences of both wells.

316 The trend of the $^{87}Sr/^{86}Sr$ ratio relative to depth is in favor of a communicating pool.
317 Not only the ratio is increasing with depth, but it is also accompanied by a continuous
318 decrease of its spread. Another argument in favor of a unique pool is the continuous decrease
319 of the elemental contents of the H_2O leachates relative to depth, as well as the reduction of
320 their spread. Both can be considered to be beyond the impact of the porosity at depth: the
321 contents have a tendency to decrease, which suggests the highest contamination in the upper
322 levels, with a quite significant spread reduction. Given as examples, the spreads of Si, Ca and
323 Sr provide similar decreasing trends relative to depth, considering that they do not represent
324 concentrations *stricto sensu,* as already stated (Fig. 6). In any case, the observed changes
325 suggest that the restored fluids were progressively less loaded with depth increase, while the
326 $^{87}Sr/^{86}Sr$ ratio increases correlatively, which favors the hypothesis of the unique pool.
327 However, this sketch does not really apply to the Sr contents that remain quite constant
328 relative to depth, except one single sample of the upper level at 2764.5 m and two samples at
329 the intermediate depths at 3116.9 and 3140.9 m of the Peciko-3 well. Also to be considered is
330 the fact that the spread of the leachates suspected to be contaminated (gray dots in Fig. 6) is
331 quite decreasing with depth.

332 Conversely, if the $^{87}Sr/^{86}Sr$ ratio would be age dependent, that is to say higher ratios
333 for older formation waters, the deepest leachates should also yield, correlatively, the higher
334 Rb contents. Indeed, higher Rb contents are expected to give the highest $^{87}Sr/^{86}Sr$ ratios
335 relative to time and consequently older "age data" for the mobile Sr in the deeper formation
336 waters, which is not the case here. The correlation among the $^{87}Sr/^{86}Sr$ and the Rb/Sr ratios
337 provides three groups of data (Fig. 10): the two upper yield the higher $^{87}Sr/^{86}Sr$ ratios with the
338 largest Rb/Sr spread for the uppermost data of the two drilling wells. Older formation waters

in the deepest grouping would also need the highest $^{87}Sr/^{86}Sr$ and Rb/Sr ratios to support a relationship induced by an age impact and this again is not the case. In summary, an older "age" for the deeper water samples seems not to be the case either.

As already stated, the $^{87}Sr/^{86}Sr$ ratios of the H_2O leachates are almost systematically higher than those of the HCl leachates, except at 2,768.1 m depth. Also, the $^{87}Sr/^{86}Sr$ ratios of both types of leachates plot farther from line of equivalent values when depth increases. The hypothesis explaining this almost systematic difference seems to combine the facts that: (1) the minerals dissolved by the dilute HCl, probably of carbonate, chloride and/or sulfate types, yield lower $^{87}Sr/^{86}Sr$ ratios than the non-contaminated pore waters of the same samples, and (2) the difference among the Sr isotopic ratios of the two leachates increases with depth. These two observations apply, in turn, to all samples of the two studied wells (Fig. 5). The differences in the Sr isotopic ratios of the successive H_2O and HCl leachates are also supportive for a crystallization of the HCl-soluble minerals before a recent flushing of pore waters, and for a progressive increase of the $^{87}Sr/^{86}Sr$ ratio relative to depth. In two cases, those of the samples at 2766.1 and 2778.7 m depth of the Peciko-3 well, the analytical uncertainties of the H_2O and HCl leachates overlap, with a large analytical uncertainty in the second case. It is, therefore, plausible that the soluble minerals and the pore waters were isotopically homogeneous once, at least for these two samples. In turn, this homogeneity being not the usual issue here, confirms that a supplementary water supply seems to have invaded the sediments after the soluble mineral crystallized and therefore very recently with a different $^{87}Sr/^{86}Sr$ ratio than that of the occurring soluble minerals. However, some interconnection between the connected samples should be visible in this case, which is not as obvious for the data of the H_2O leachates from two wells.

5.3. The meaning of the REE contents and patterns in the H_2O leachates

It is probably appropriate to recall here that REEs are lithophyte, electropositive, mostly trivalent and refractory. Their use in geochemistry is based on systematic variations of their ionic radius, as well as on the complexion capacities of two of them to change their redox state: cerium as Ce^{3+} and Ce^{4+}, and europium as Eu^{2+} and Eu^{3+}. Also to be remembered is the fact that REE patterns characterizing sedimentary materials are often very uniform as they are representative of the upper continental crust (Taylor and McLennan, 1985), which is easily tested by comparing any REE spectrum to the pattern of the PAAS reference. These patterns are usually identified by a negative Eu anomaly due to varied oxidation-reduction conditions and a more or less positive Eu anomaly that focuses specifically on some

partitioning of detrital plagioclases that were progressively altered. In this context, seawater is generally characterized by marked Ce depletions due to an oxidation into Ce^{IV} and its separation from other REE by preferential uptake onto Mn^{IV} oxide.

The REE patterns characterized by low to very low contents display scattered distributions relative to the PAAS, which is partly due to analytical aspects inherent for extremely low contents (Fig. 9, lower row). The patterns also yield a systematic irregular increase from Eu to Gd and Tb, as well as a systematic low La/Yb ratio. The low to very low total REE contents relative to depth include almost automatically REEs with contents below the detection limit. The fact that fluids contain usually very low contents of REEs makes that the primary role of these REEs is here in the detection of a contamination of the pore waters by their abnormally high contents in the H_2O leachates. Together with high metal contents, they allow identifying and discarding the contaminated waters. It might be added that increased contents of heavy REEs could also be theoretically due to the use of surface water during drilling that diffused into the sandy matrix with the drilling pollutants. On the basis of these constraints, twelve H_2O leachates of the Peciko-3 well remain eligible for representing the restored pore waters, as well as four leachates of the Peciko-8 well. In the former drilling, they were collected close to 2,737 and 2,747 m in the upper part, between 3,118 and 3,183 m in the intermediate level, and the five deepest samples. Four leachates from second drilling well are also in these values: that close to 3,506 m and the three deepest samples between 3,534 and 3,538 m depth.

If now one considers the $^{87}Sr/^{86}Sr$ ratio of the non-contaminated H_2O leachates, it is clear that the two uppermost clean water samples are not in continuous connection and that they seem, with lower Sr isotopic values, to have been mixed with present-day surface waters. In the intermediate sequence, the four samples located between about 3,118 and 3,177 m depth could be part of a communicating pool, while the deepest leachates of the Peciko-3 well seem to be presently isolated with the highest $^{87}Sr/^{86}Sr$ ratios of the whole water sequence. Also none of the highest Sr isotopic data from deepest leachates of the second drilling well overlap and, therefore, are probably not connected directly.

5.4. The meaning of the combined elemental contents and Sr isotopic signatures

The HCl leaching dissolved carbonates and sulfates that crystallized either during the recent invasion of the pore waters or previously to it. This second hypothesis is the most appropriate as the two types of leachates yield almost never the same $^{87}Sr/^{86}Sr$ ratio. Not contemporaneous with the current pore waters, the HCl soluble minerals precipitated then

probably before the present-day fluids diffused into the sediments. In fact, identical $^{87}Sr/^{86}Sr$ ratios for the two types of leachates was only obtained at 2,766 and 2,779 m depth, where the soluble minerals could be somehow contemporaneous with the pore waters, both with $^{87}Sr/^{86}Sr$ ratios within analytical uncertainty.

Restoring pore waters of sediments is analytically quite easy. However, the restored fluids appear more sensitive to contamination than the associated soluble minerals, at least here. To test such anthropogenic pollution, the REE contents of the restored waters seem to be an appropriate basis to discard those fluids containing large amounts of REEs, together with high metal contents. Beyond these analytical aspects that are useful in the selection of samples representative of "natural" environments, the $^{87}Sr/^{86}Sr$ ratios of restored waters also represent an efficient tool to trace the connectivity of superposed pore-water systems. Here in the case of the Peciko gas field, the superposed channelizing horizons seem not to be often interconnected, at least nearby the drilling wells, unless drilling cemented somehow the sands around. Such characteristics are also of interest if a reservoir field is studied for potential CO_2 storage for instance.

6. Conclusions

In an attempt to restore the pore waters of the hydrocarbon-bearing sand units from Peciko gas reservoir in the southern Mahakam Delta (Indonesia), the host rocks were leached with de-ionized water to analyze the major, trace and rare earth elemental contents of the separates with the $^{87}Sr/^{86}Sr$ ratios. After water leaching, the rocks were also treated with dilute hydrochloric acid to analyze the $^{87}Sr/^{86}Sr$ ratios of the associated soluble minerals.

Abnormally high REE and metal contents suggest that most of the recovered H_2O leachates were contaminated, most probably during drilling. The $^{87}Sr/^{86}Sr$ ratios of the non-polluted leachates increase progressively with depth, suggesting in turn that the pore waters from upper sandy layers were mixed, probably recently, with local waters of riverine origin. Also, only a few water levels at intermediate depths yield analytically similar $^{87}Sr/^{86}Sr$ ratios suggesting interconnections. On the other hand, the minerals that were dissolved by dilute hydrochloric acid yield quite systematically lower $^{87}Sr/^{86}Sr$ ratios than the associated pore waters. These minerals most probably crystallized before the invasion of the sedimentary sequence by recent to present-day pore waters. Also, the superposed pore-water horizons seem not to have been interconnected in the gas field, at least near the drilling wells.

7. Acknowledgements

Sincere thanks are for Dr. F. Sommer of the French Total-SA oil company who provided the samples, some corresponding information as well as a financial support for the technical realization of this study. We had numerous interactions over the years until he retired some years ago. Dr. S. Furlan, as a young post-doctoral collaborator at the time deserves also thanks for her active contribution during this study, especially in the preparation of the material to be analyzed. Sincere thanks are also for an anonymous reviewer whose comments were very helpful improving the presentation of the data, as well as the discussion. At last but not least, J. Samuel and R. Rouault engineers at the time of the Centre de Géochimie de la Surface of the University Louis Pasteur at Strasbourg are also thanked for their contribution to the analytical procedure.

8. References

Banner, J.L., Wasserburg, G.J., Dobson, P.F., Carpenter, A.B. and Moore, C.H., 1989. Isotopic and trace element constraints on the origin and evolution of saline groundwaters from central Missouri. Geochim. Cosmochim. Acta 53, 383-398.

Burrus, J., Brosse, E., Chopin de Janvry, G., Grosjean, Y. and Oudin, J.L., 1992. Basin modeling in the Mahakam Delta based on the integrated 2D model Temispack. Proceedings I.P.A., 21st Ann. Conv. 1, 23-43.

Carpenter, A.B., 1978. Origin and chemical evolution of brines in sedimentary basins. Okla. Geol. Surv. Circ. 79, 60-77.

Chaudhuri, S., 1978. Strontium isotopic composition of several oilfield brines from Kansas and Colorado. Geochim. Cosmochim. Acta 42, 329-331.

Chaudhuri, S., Clauer, N. and O'Neil, J.R., 1983. Hydrogeochemical evolution of some oil-field waters from central Kansas (USA). Terr. Cogn. 3, 177-178.

Chaudhuri, S., Broedel, V. and Clauer, N., 1987. Strontium isotopic evolution of oil-field waters from carbonate reservoir rocks in Bindley field, central Kansas, U.S.A. Geochim. Cosmochim. Acta 51, 45-53.

Clayton, R.N., Friedman, I., Graf, D.L., Mayeda, T.K., Meents, W.F. and Shump, N.F., 1966. The origin of saline formation waters. 1. Isotopic composition. J. Geophys. Res. 71, 3869-3882.

Collins, A.G.. 1975. Geochemistry of Oilfield Waters. Elsevier Scientific Publishing Company, Amsterdam, 343-364.

Degens, E.T, Hunt, J.M., Reuter ,J.H. and Reed, W.E., 1964. Data on the distribution of amino acids and oxygen isotopes in petroleum brine waters of various geologic ages. Sediment. 3, 199-225.

De Sitter, L.U., 1947. Diagenesis of oil-field brines. Amer. Assoc. Petrol. Geol. Bull. 31, 2030-2047.

Duval, B.C., Choppin de Janvry, G. and Loiret, B., 1992. The Mahakam Delta Province: an ever-changing picture and a bright future. 24th Ann. Offshore Technol. Conf., Houston Texas, May 7 1992, 393-404.

Furlan, S., Chaudhuri, S., Clauer, N. and Sommer, F., 1995. Geochemistry of formation waters and hydrodynamic evolution of a young and restricted sedimentary basin (Mahakam Delta Basin, Indonesia). Basin Res. 7, 9-20.

Grosjean, Y., Choppin de Janvry, G. and Duval, B.C., 1994. Discovery of a giant in a mature deltaic province: Peciko, Indonesia. 14th World Petrol. Cong., May 29-June 1, 1994, Stavanger, Norway, 4p.

Hitchon, B., Billings, G.A. and Klovan, J.E., 1971. Geochemistry and origin of formation waters in the western Canada sedimentary basin - III. Factors controlling chemical composition. Geochim. Cosmochim. Acta 35, 567-598.

Kharaka, Y.K., Berry, F.A.F. and Friedman, I., 1973. Isotopic composition of oil-field brines from Kettleman North Dome, California and their geologic implications. Geochim. Cosmochim. Acta 37, 1899-1908.

Kharaka, Y.K. and Berry, F.A.F., 1974. The influence of geological membranes on the geochemistry of subsurface waters from Miocene sediments at Kettleman North Dome in California. Water Res. 10, 313-327.

Letouzey, J., Werner, P. and Marty, A., 1990. Fault reactivation and structural inversion. Backarc and intraplate compressive deformations. Example of the eastern Sunda shelf (Indonesia). Tectonoph. 183, 341-362.

McArthur, J.M., Howarth, R.J. and Bailey, T.R., 2001. Strontium isotope stratigraphy: LOWESS Version 3: Best fit to the marine Sr-isotope curve 0-509 Ma and accompanying look-up table for deriving numerical age. J. Geol. 109, 155-170.

Rittenhouse, G., 1967. Bromine in oil-field waters and its use in determining possibilities of origin of these waters. Am. Ass. Petrol. Geol. Bull. 51, 2430-2440.

Samuel, J., Rouault, R. and Besnus, Y., 1985. Analyse multi-élémentaire standardisée des matériaux géologiques en spectrométrie d'émission par plasma à couplage inductif. Anal. 13, 312-317.

Schaltegger, U., Stille, P., Rais, N., Piqué, A. and Clauer, N., 1994. Nd and Sr isotopic dating of diagenesis and low-grade metamorphism of argillaceous sediments. Geochim. Cosmochim. Acta 58, 1471-1481.

Starinsky, A., Bielski, M., Lazar, B., Steinitz, G. and Raab, M., 1983. Strontium isotope evidence on the history of oilfield brines, Mediterranean Coastal Plain, Israel. Geochim. Cosmochim. Acta 47, 687-695.

Stueber, A.M., Pushkar, P. and Hetherington, E.A., 1984. A strontium isotopic study of Smackover brines and associated solids, southern Arkansas. Geochim. Cosmochim. Acta 48, 1637-1649.

Stolum, H.H., Smalley, P.C. and Hanken, N.M., 1993. Prediction of large-scale communication in the Smorbukk fields from strontium fingerprinting. ln: Petroleum Geology of Northwest Europe, Parker J.R. (Ed.), Proceedings of the 4th Conference 1421-1432.

Stones, D.S and Hoeger, R.L., 1973. Importance of Hydrodynamic Factor in Formation of Lower Cretaceous Combination Traps, Big Muddy-South Glenrock Area, Wyoming. Amer. Assoc. Petrol. Geol. Bull. 57, 1714-1733.

Sulin, V.A., 1947. Waters of petroleum formations in the system of natural waters. Gostopekhizdat, Moscow, 35-96.

Sunwall, M.T. and Pushkar, P., 1979. The isotopic composition of strontium in brines from petroleum fields of southeastern Ohio. Chem. Geol. 24, 189-197.

Taylor, S.R. and McLennan, S.M., 1985. The Continental Crust; Its composition and evolution; an examination of the geochemical record preserved in sedimentary rocks. Blackwell, Oxford 312.

White, C.E., 1965. Saline waters of sedimentary rocks. In: Fluids in sub-surface environments, Young A. and Galley J.E. (Eds.), Amer. Ass. Petrol. Geol. Mem. 4, 324-336.

Table and figure captions

Figure 1: Location of the Peciko gas field in the Mahakam delta (modified from Furlan et al., 1995).

Figure 2: North-to-South cross section of the northern Peciko gas field. The cross section illustrates the reservoir units (in black) between the Peciko-3 and Peciko-8 drillings. In the upper zone they are sub-horizontal towards the North and sub-vertical to the South.

In the lower zone, they are tilted in both flanks and steeper to the South (modified from Grosjean et al., 1994).

Figure 3: The $^{87}Sr/^{86}Sr$ ratios relative to the corresponding Rb/Sr ratios of the H_2O leachates from Peciko-3 well in the diagram (A) and from Peciko-8 well in the diagram (B). The depths of the samples with data points away from the lines are given next to the dots.

Figure 4: The $^{87}Sr/^{86}Sr$ ratios of the H_2O and HCl leachates relative to depth in the two Peciko drillings. The data of the Peciko-3 well are to the left and those of the Peciko-8 well are to the right. The two upper diagrams display the $^{87}Sr/^{86}Sr$ ratios of the H_2O leachates and the two lower those of the HCl leachates.

Figure 5: The $^{87}Sr/^{86}Sr$ ratios of the H_2O vs. HCl leachates relative to depth in the Peciko-3 (A) and in the Peciko-8 (B) drill wells.

Figure 6: The contents of four major elements of the H_2O leachates relative to depth in the Peciko-3 well (in the four upper diagrams) and of Rb and Sr (in the two lower diagrams). The arrows (full and dashed) underline the spread of the data relative to collection depth. The leachates susceptible to have been contaminated are shown by the gray dots.

Figure 7: Elemental ratios of six major and two trace elements of the H_2O leachates relative to depth in the Peciko-3 well.

Figure 8: The contents of three metal-trace elements of the H_2O leachates relative to depth in the Peciko-3 well. The arrows (full and dashed) underline the spread of the data relative to collection depth.

Figure 9: The REE patterns of the H_2O leachates relative to the PAAS reference. The numbers below each diagram stand for the REEs from La to Lu and the dashed lines are drafted to show the graphic relation between the two REE end members.

Figure 10: The $^{87}Sr/^{86}Sr$ ratios relative to the corresponding Rb/Sr ratios of the H_2O leachates from Peciko-3 well in the diagram (A) and from Peciko-3 well in the diagram (B). The depths of the samples with data points away from the lines are given next to the dots.

Table 1: The contents in major elements of the H_2O leachates.

Table 2: The contents in trace elements of the H_2O leachates.

Table 3: The contents in rare-earth elements of the H_2O leachates.

Table 4: The $^{87}Sr/^{86}Sr$ ratios of the H_2O and HCl leachates and the difference in the $^{87}Sr/^{86}Sr$ ratios of both in the same leachates at the same depths.

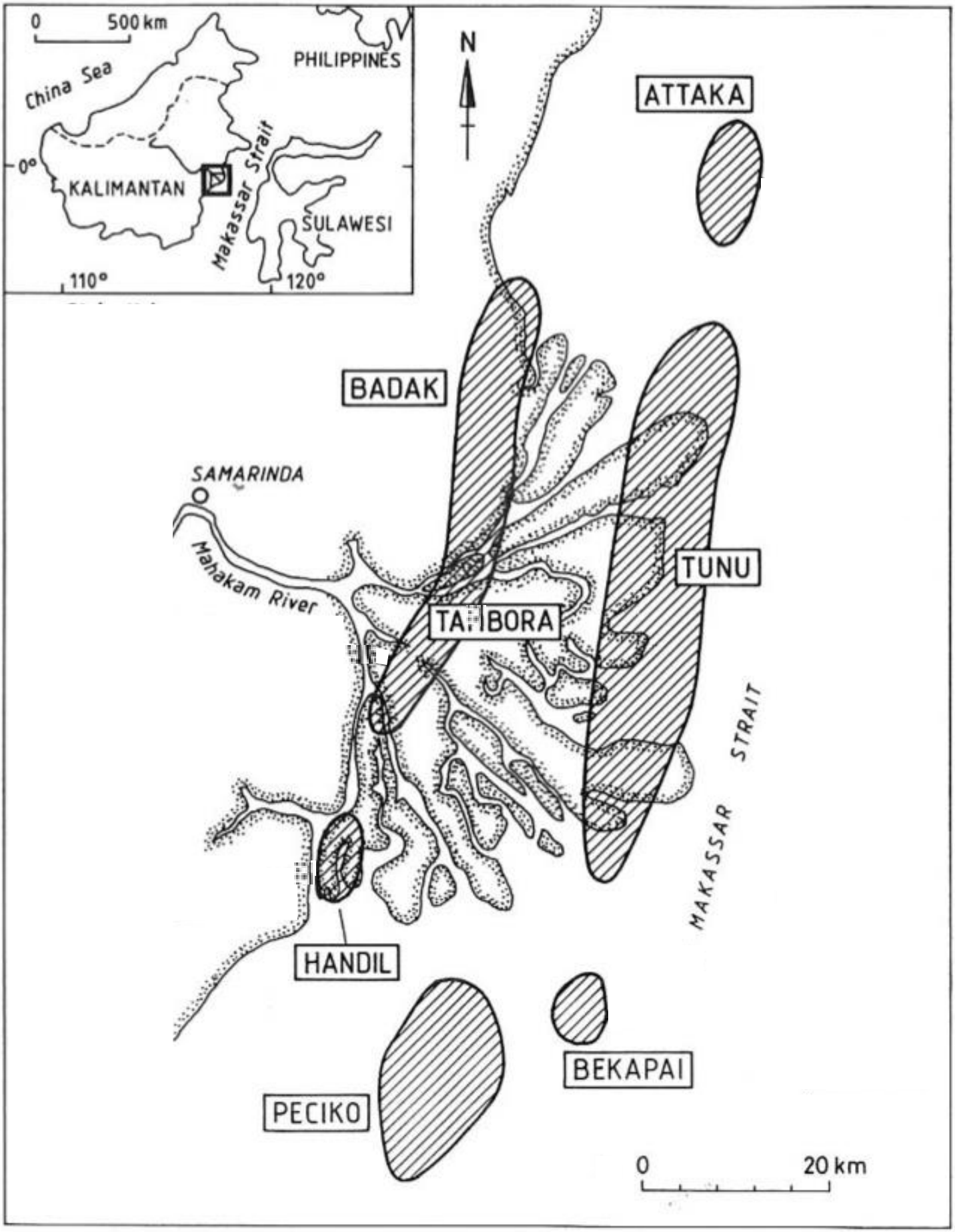
0 500 km
China Sea
PHILIPPINES
0°
KALIMANTAN
Makassar Strait
SULAWESI
110°
120°
N
ATTAKA
BADAK
SAMARINDA
Mahakam River
TUNU
TABORA
MAKASSAR STRAIT
HANDIL
BEKAPAI
PECIKO
0 20 km

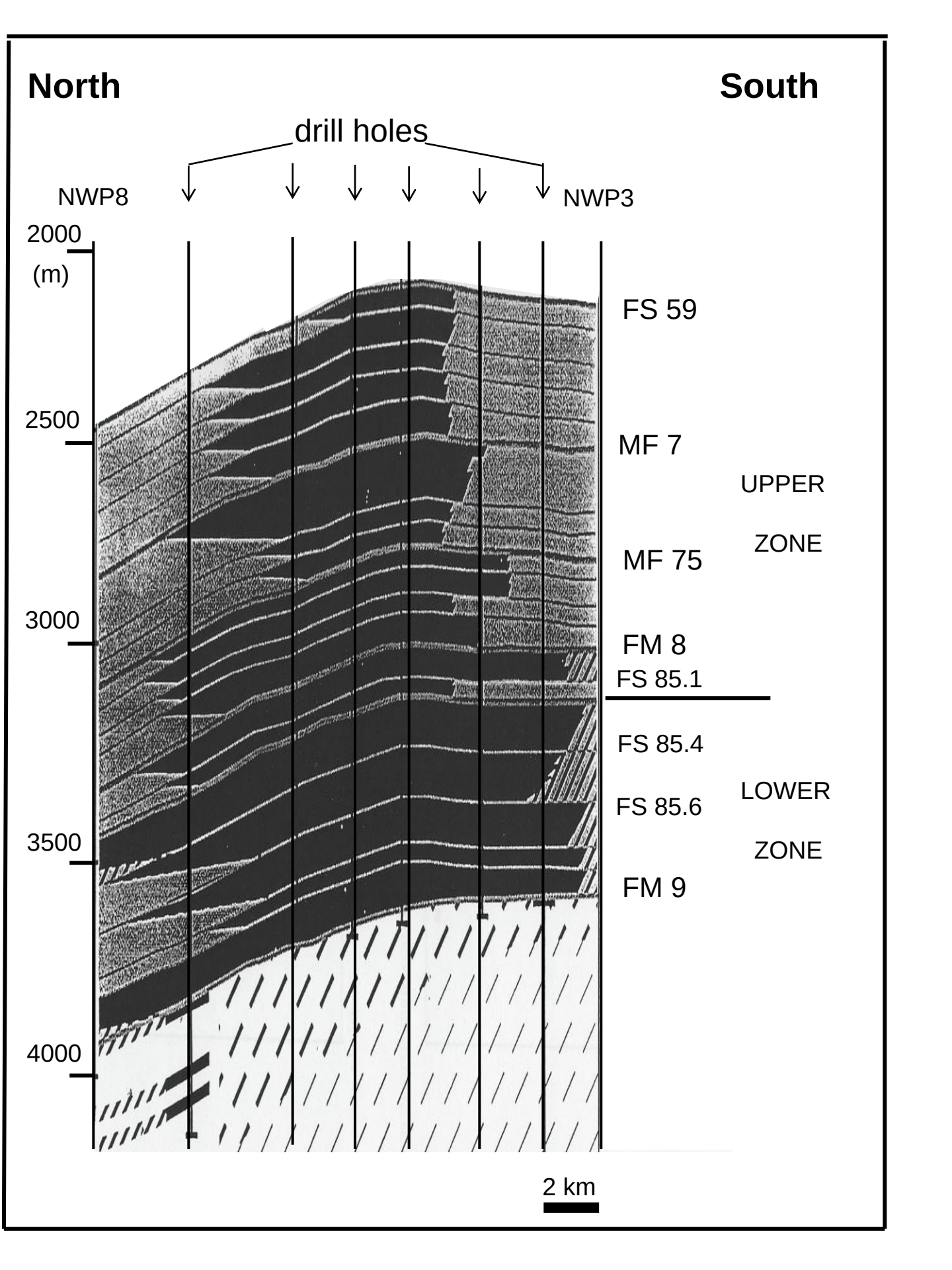
North
South
drill holes
NWP8
NWP3
2000
(m)
2500
3000
3500
4000
FS 59
MF 7
UPPER
ZONE
MF 75
FM 8
FS 85.1
FS 85.4
LOWER
FS 85.6
ZONE
FM 9
2 km

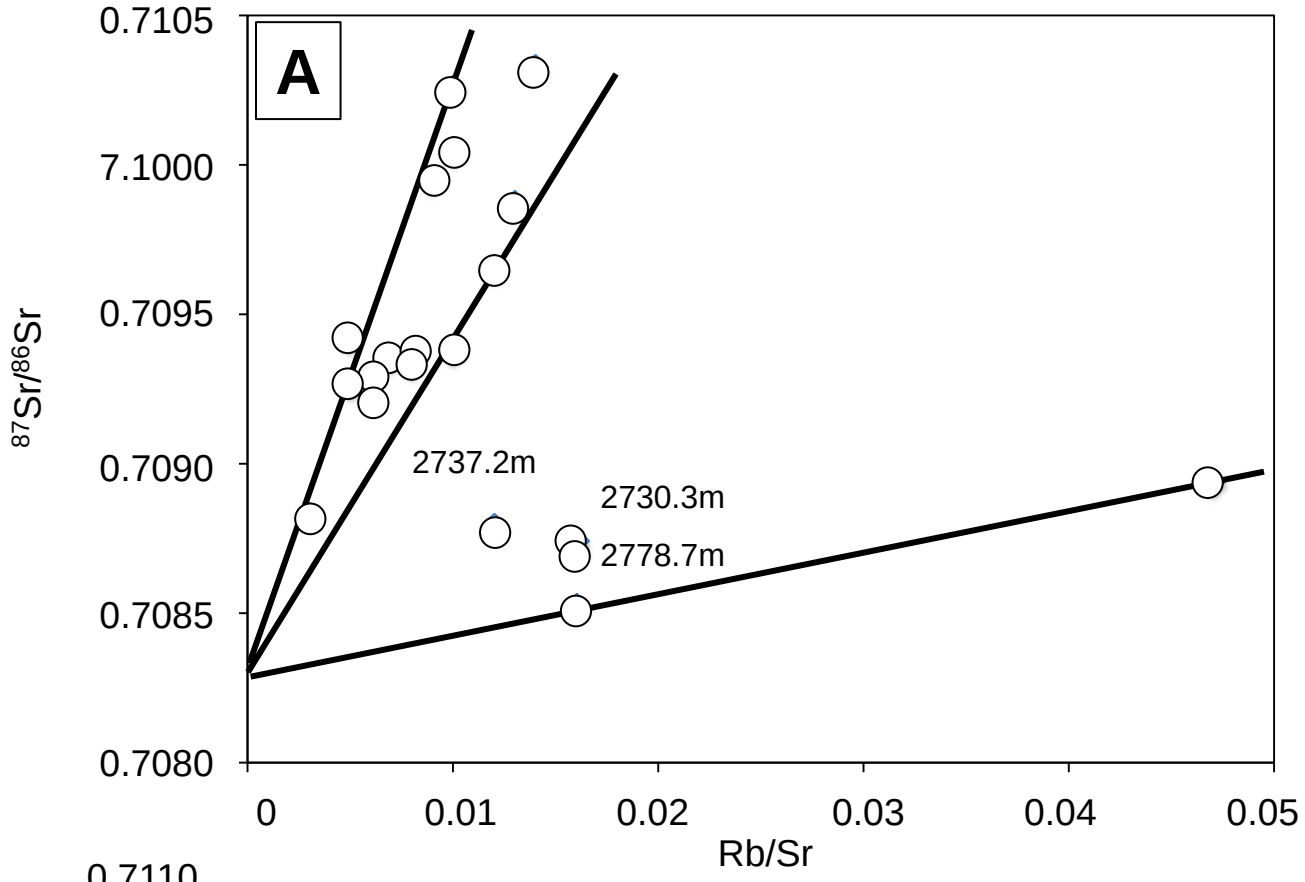
A
0.7105
7.1000
0.7095
0.7090
0.7085
0.7080
$^{87}Sr/^{86}Sr$
2737.2m
2730.3m
2778.7m
0
0.01
0.02
0.03
0.04
0.05
Rb/Sr

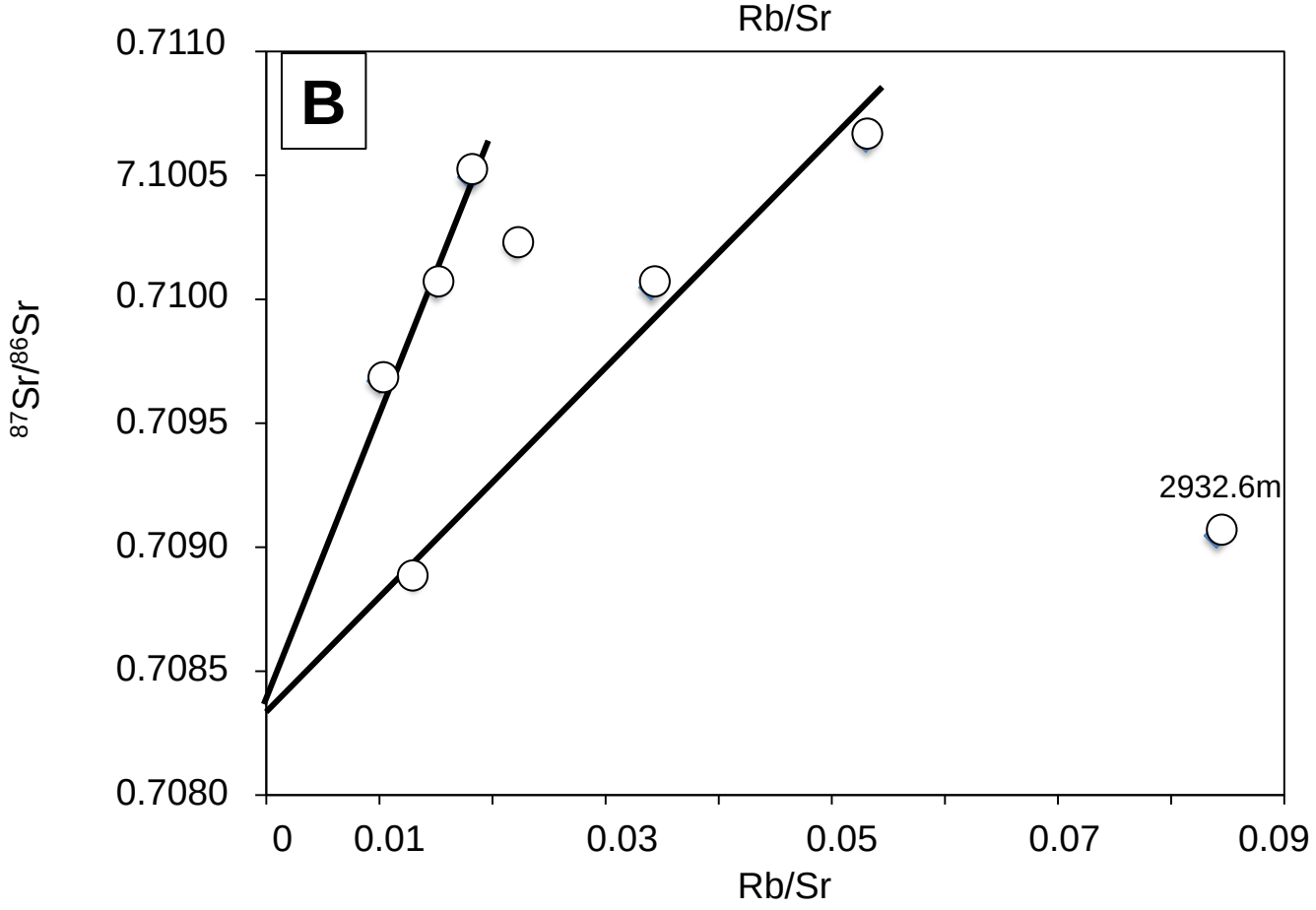
B
0.7110
7.1005
0.7100
0.7095
0.7090
0.7085
0.7080
$^{87}Sr/^{86}Sr$
2932.6m
0
0.01
0.03
0.05
0.07
0.09
Rb/Sr

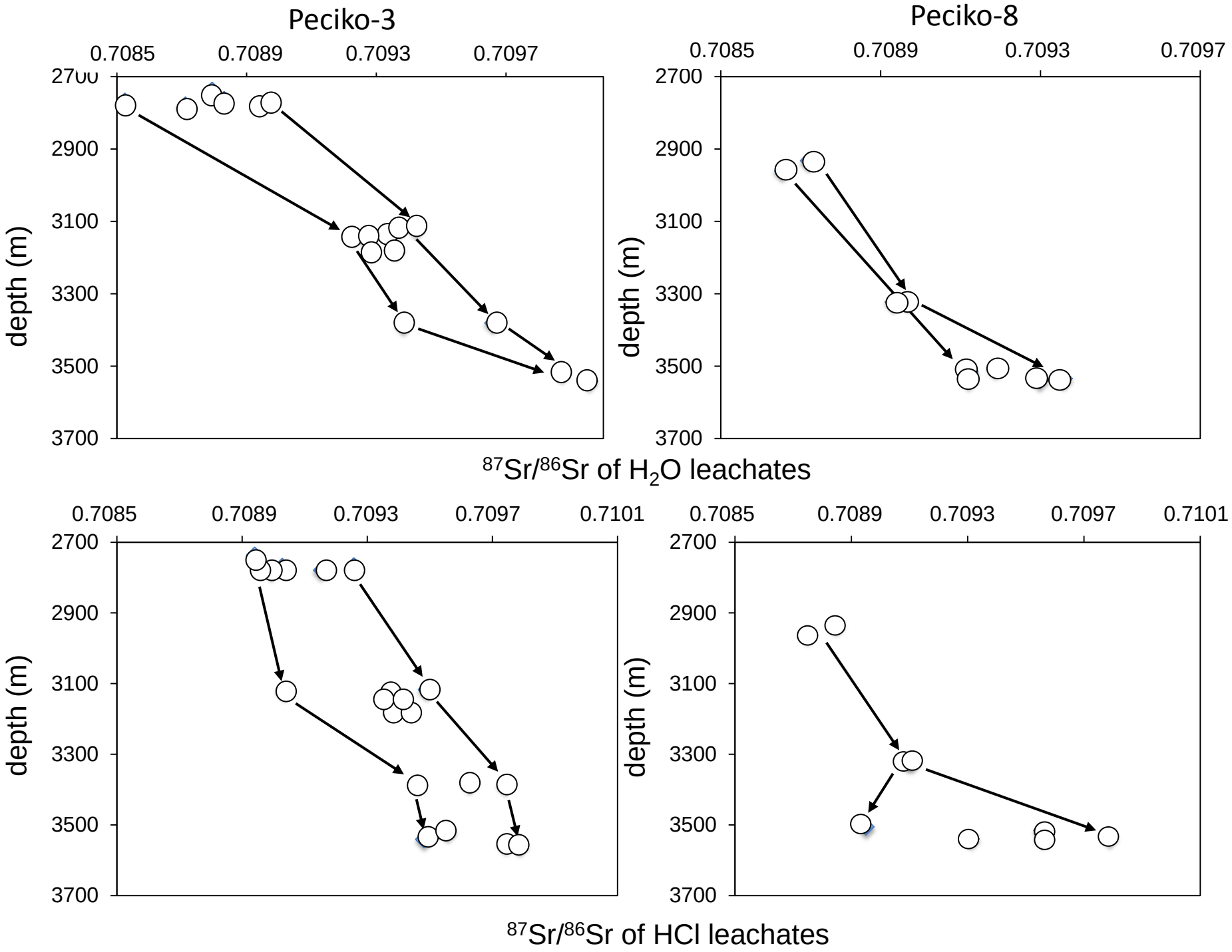
Peciko-3
Peciko-8
0.7085
0.7089
0.7093
0.7097
0.7101
2700
2900
3100
3300
3500
3700
depth (m)
$^{87}Sr/^{86}Sr$ of H_2O leachates
$^{87}Sr/^{86}Sr$ of HCl leachates

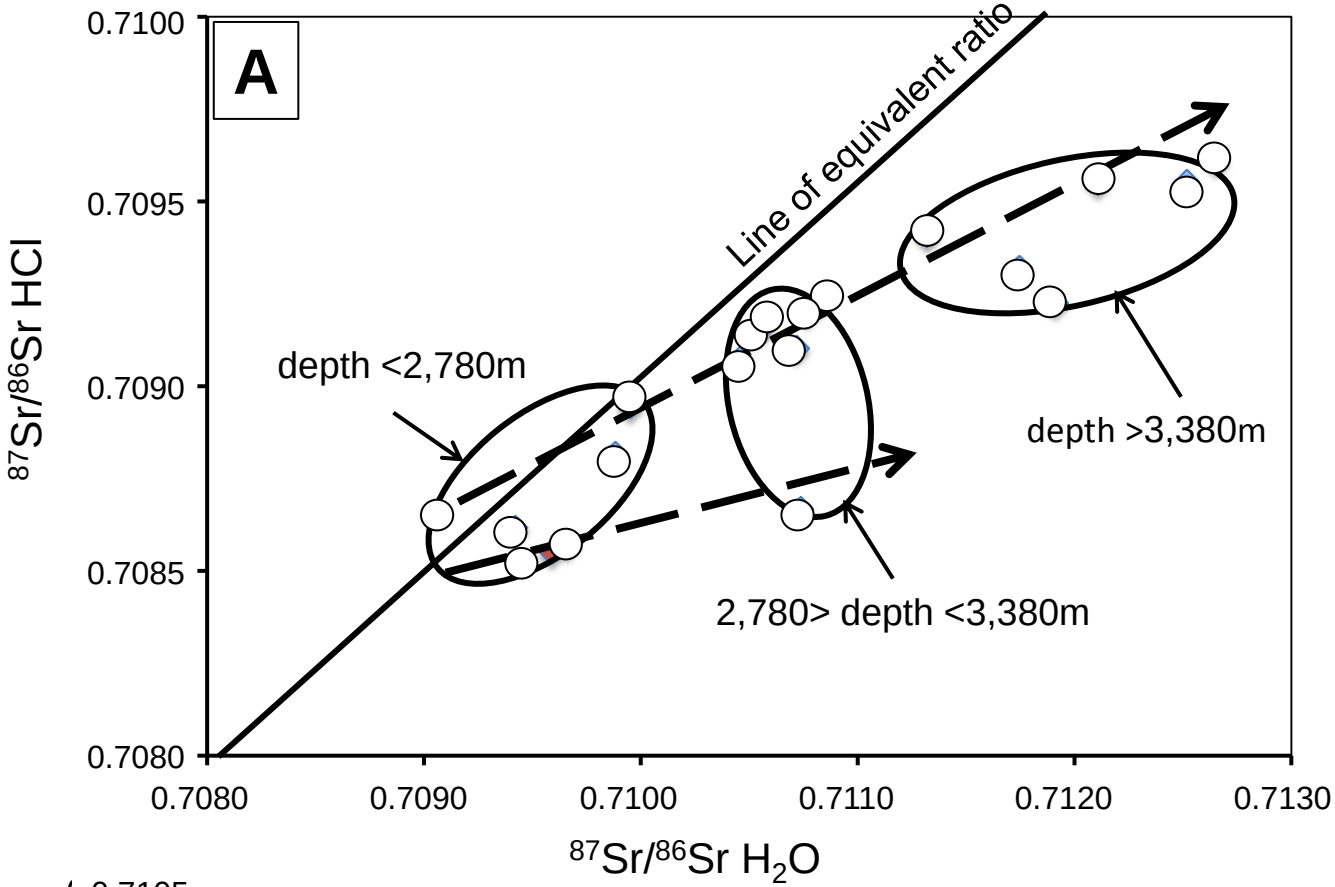
A
0.7100
0.7095
0.7090
0.7085
0.7080
$^{87}Sr/^{86}Sr$ HCl
Line of equivalent ratio
depth <2,780m
depth >3,380m
2,780> depth <3,380m
0.7080
0.7090
0.7100
0.7110
0.7120
0.7130
$^{87}Sr/^{86}Sr$ H_2O

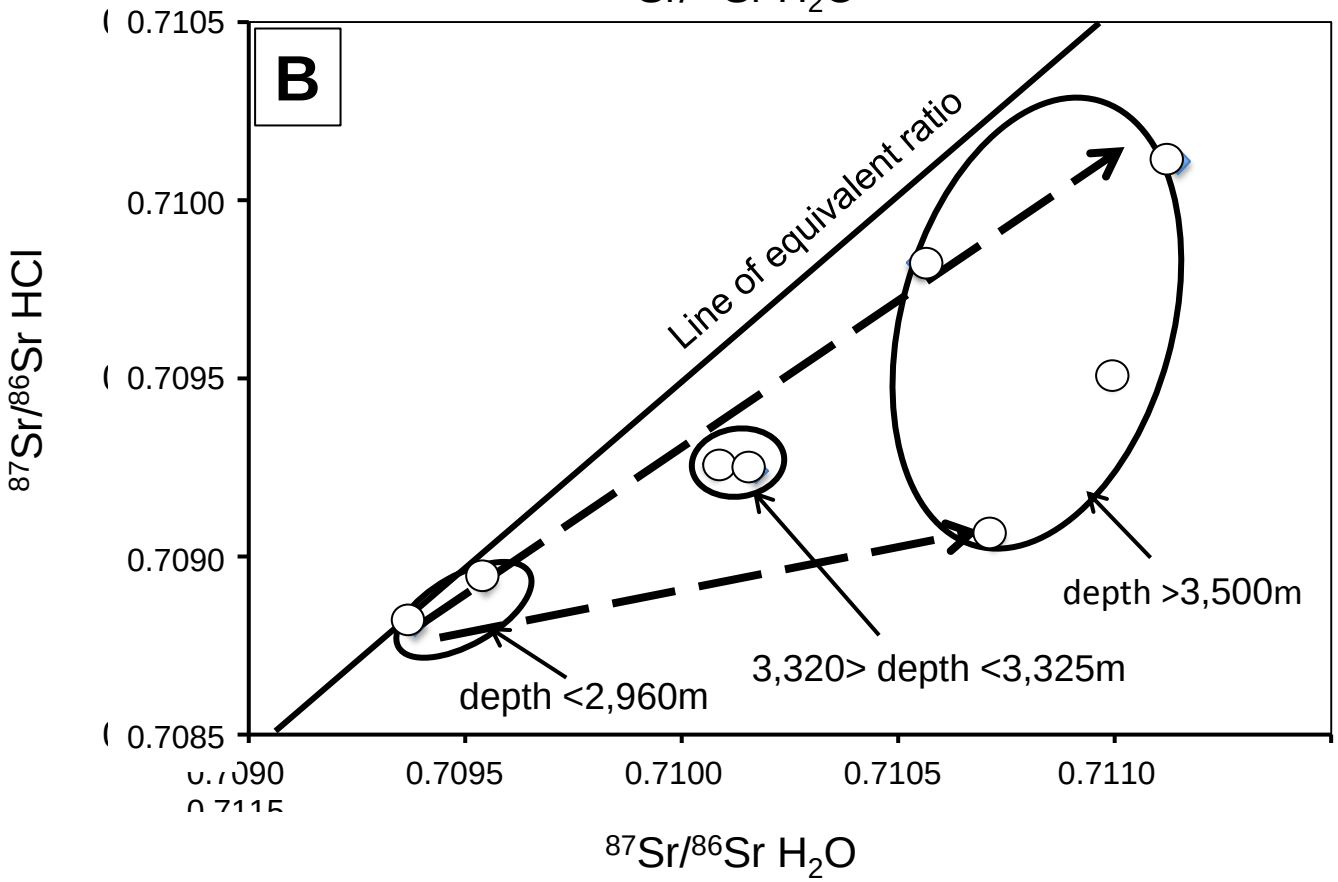
B
0.7105
0.7100
0.7095
0.7090
0.7085
$^{87}Sr/^{86}Sr$ HCl
Line of equivalent ratio
depth >3,500m
3,320> depth <3,325m
depth <2,960m
0.7090
0.7095
0.7100
0.7105
0.7110
$^{87}Sr/^{86}Sr$ H_2O

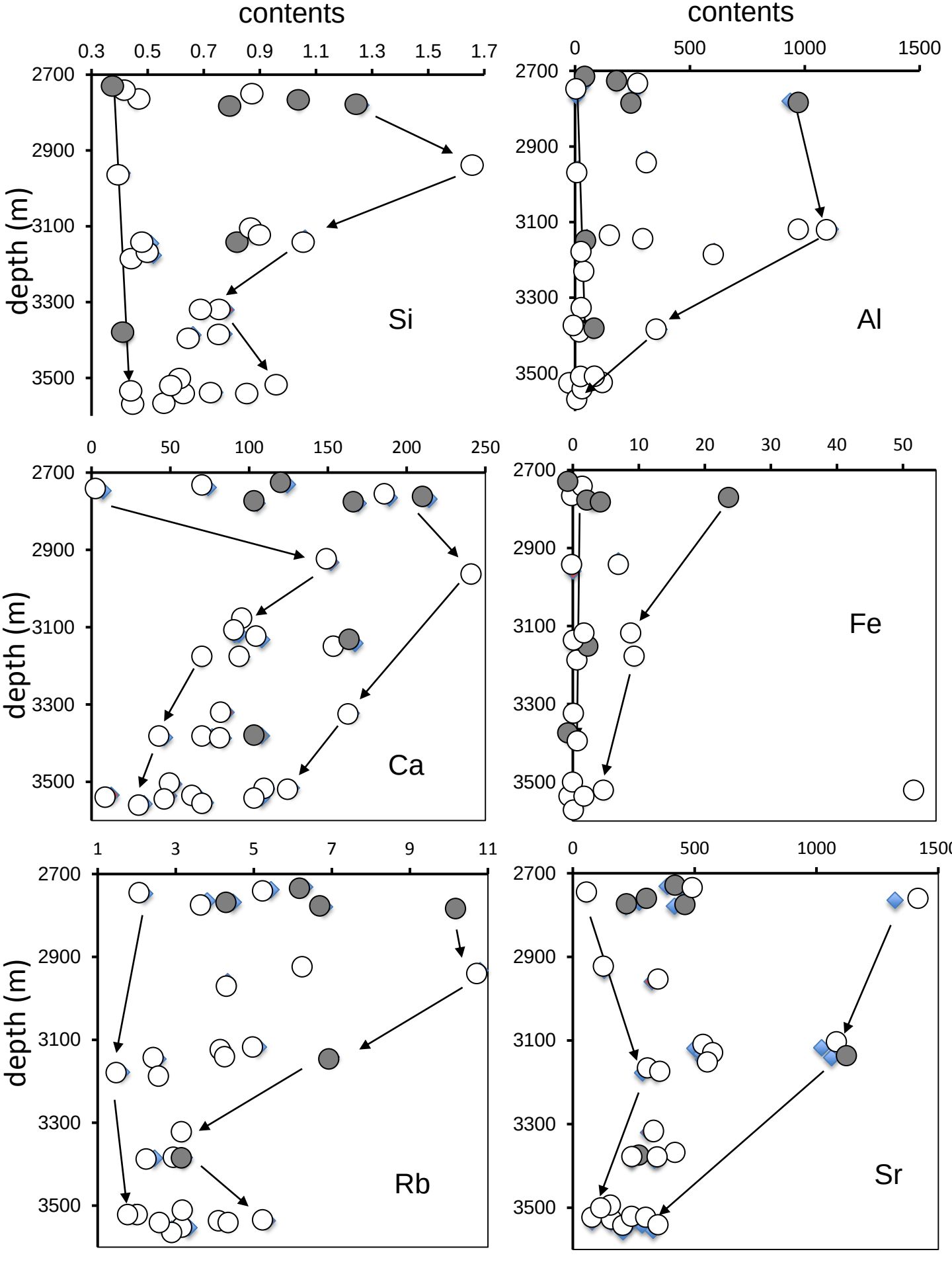
contents
0.3
0.5
0.7
0.9
1.1
1.3
1.5
1.7
2700
2900
3100
3300
3500
depth (m)
Si
contents
0
500
1000
1500
Al
0
50
100
150
200
250
Ca
0
10
20
30
40
50
Fe
1
3
5
7
9
11
Rb
0
500
1000
1500
Sr

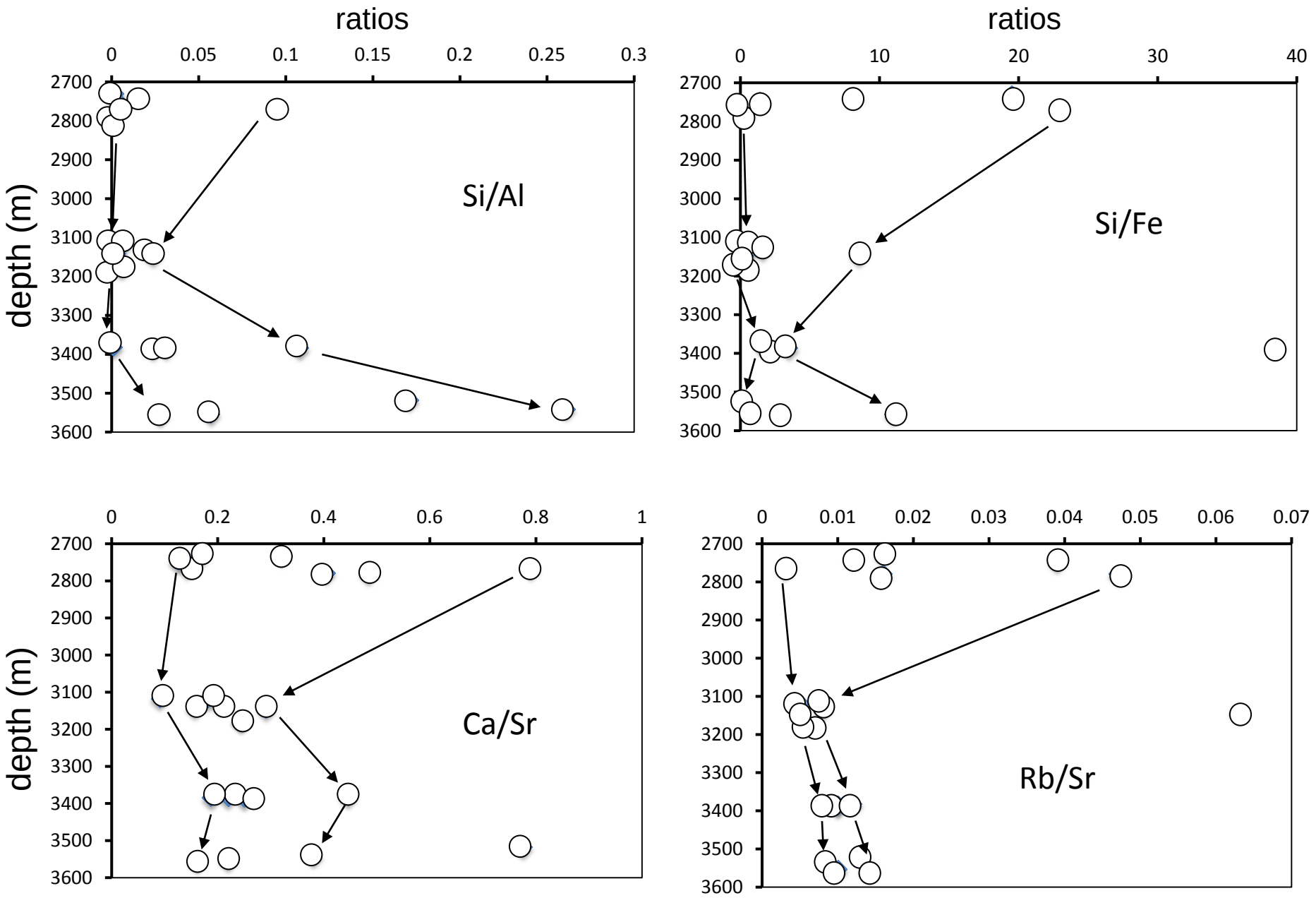
ratios
0
0.05
0.1
0.15
0.2
0.25
0.3
depth (m)
2700
2800
2900
3000
3100
3200
3300
3400
3500
3600
Si/Al
ratios
0
10
20
30
40
Si/Fe
0
0.2
0.4
0.6
0.8
1
Ca/Sr
0
0.01
0.02
0.03
0.04
0.05
0.06
0.07
Rb/Sr

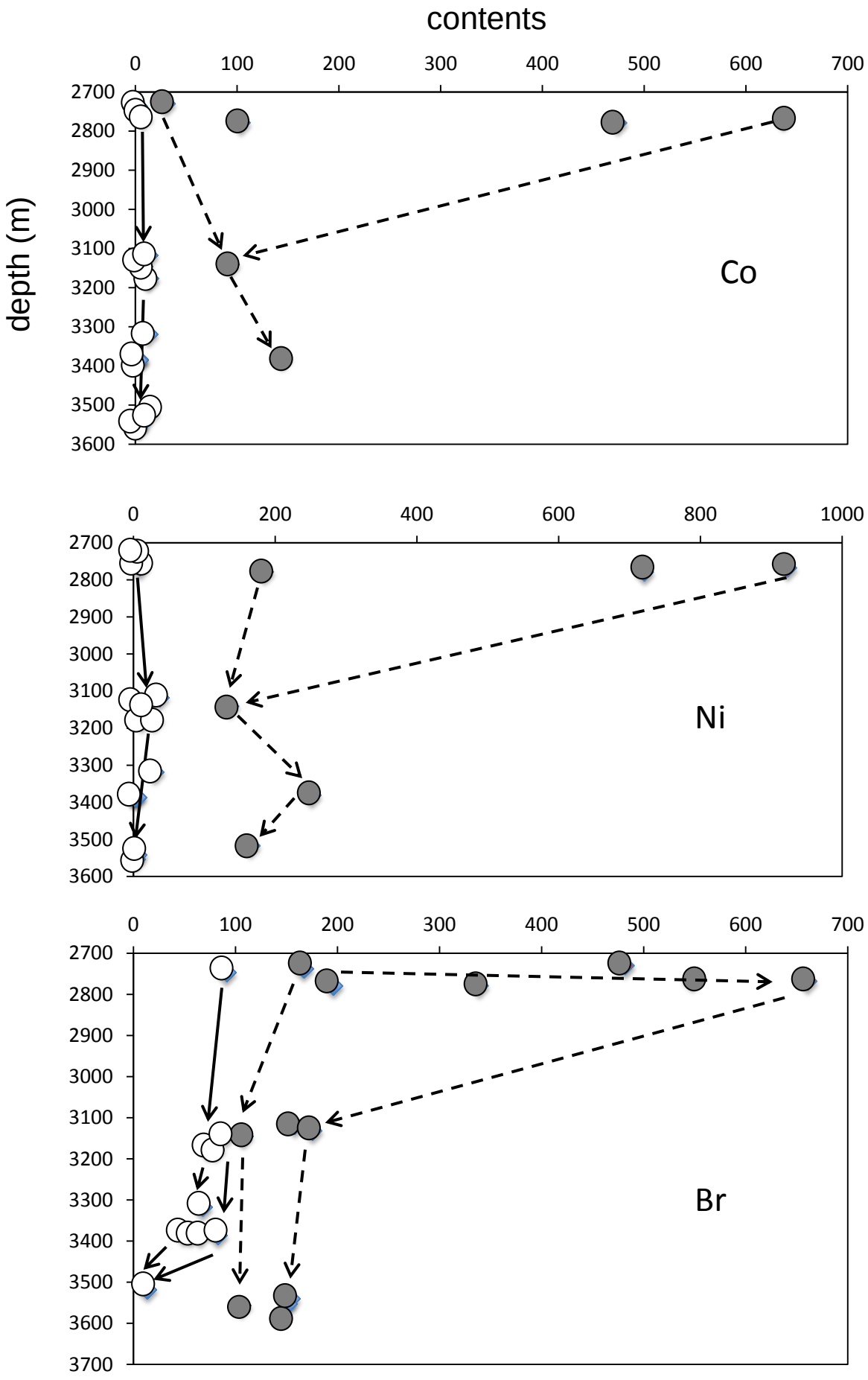
contents
depth (m)
0
100
200
300
400
500
600
700
2700
2800
2900
3000
3100
3200
3300
3400
3500
3600
Co
0
200
400
600
800
1000
2700
2800
2900
3000
3100
3200
3300
3400
3500
3600
Ni
0
100
200
300
400
500
600
700
2700
2800
2900
3000
3100
3200
3300
3400
3500
3600
3700
Br

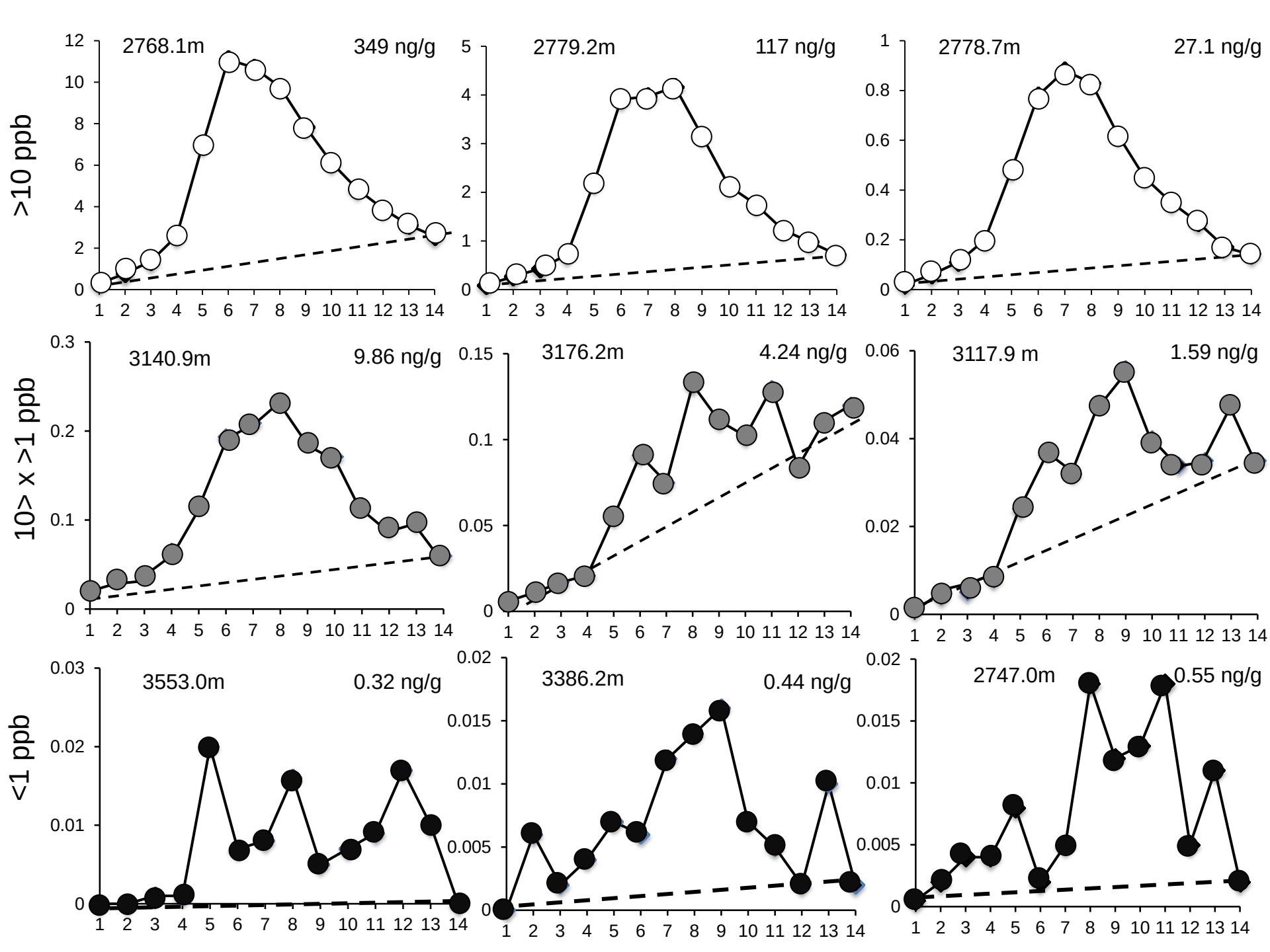
>10 ppb
10> x >1 ppb
<1 ppb
2768.1m
349 ng/g
2779.2m
117 ng/g
2778.7m
27.1 ng/g
3140.9m
9.86 ng/g
3176.2m
4.24 ng/g
3117.9 m
1.59 ng/g
3553.0m
0.32 ng/g
3386.2m
0.44 ng/g
2747.0m
0.55 ng/g

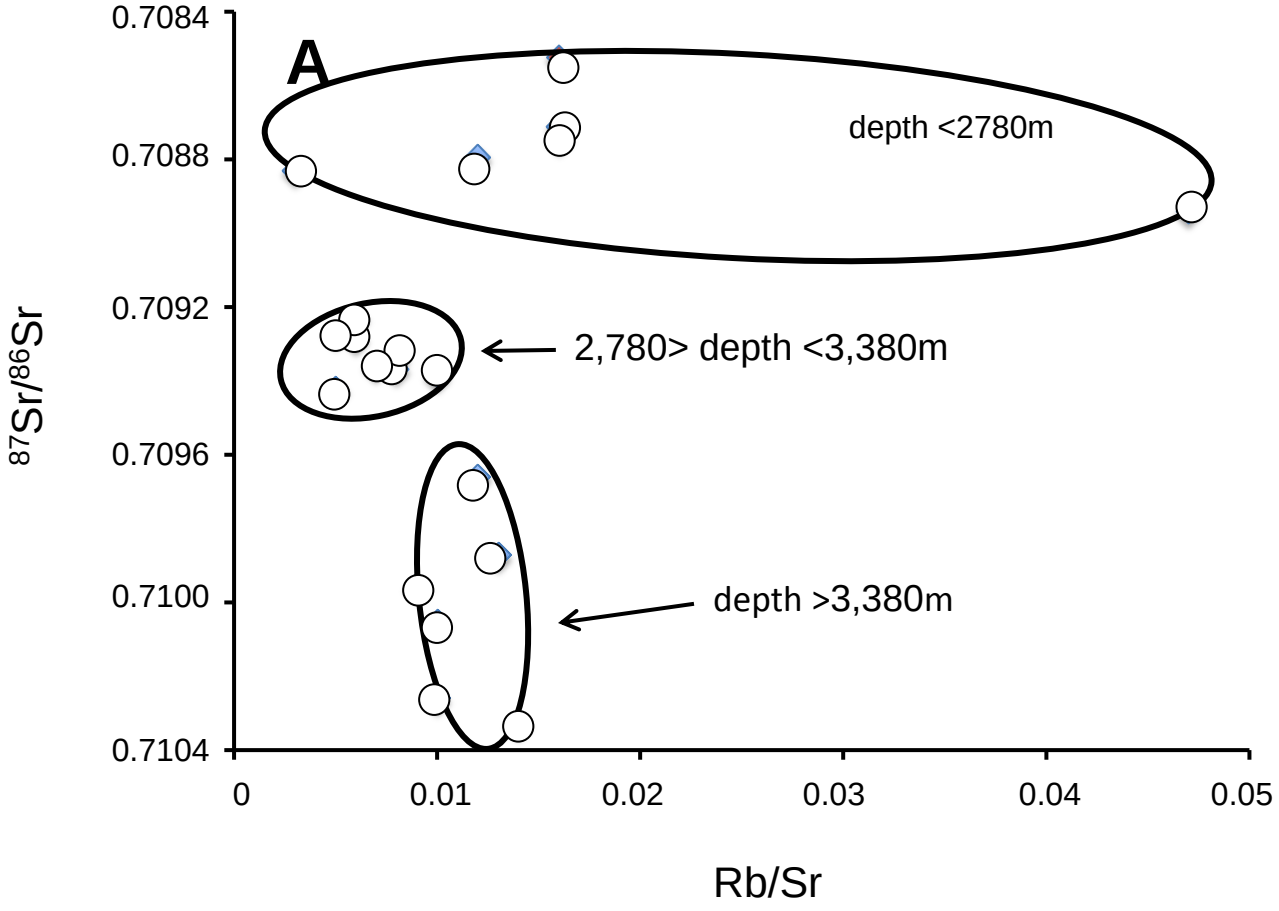
A
0.7084
0.7088
0.7092
0.7096
0.7100
0.7104
$^{87}Sr/^{86}Sr$
depth <2780m
2,780> depth <3,380m
depth >3,380m
0
0.01
0.02
0.03
0.04
0.05
Rb/Sr

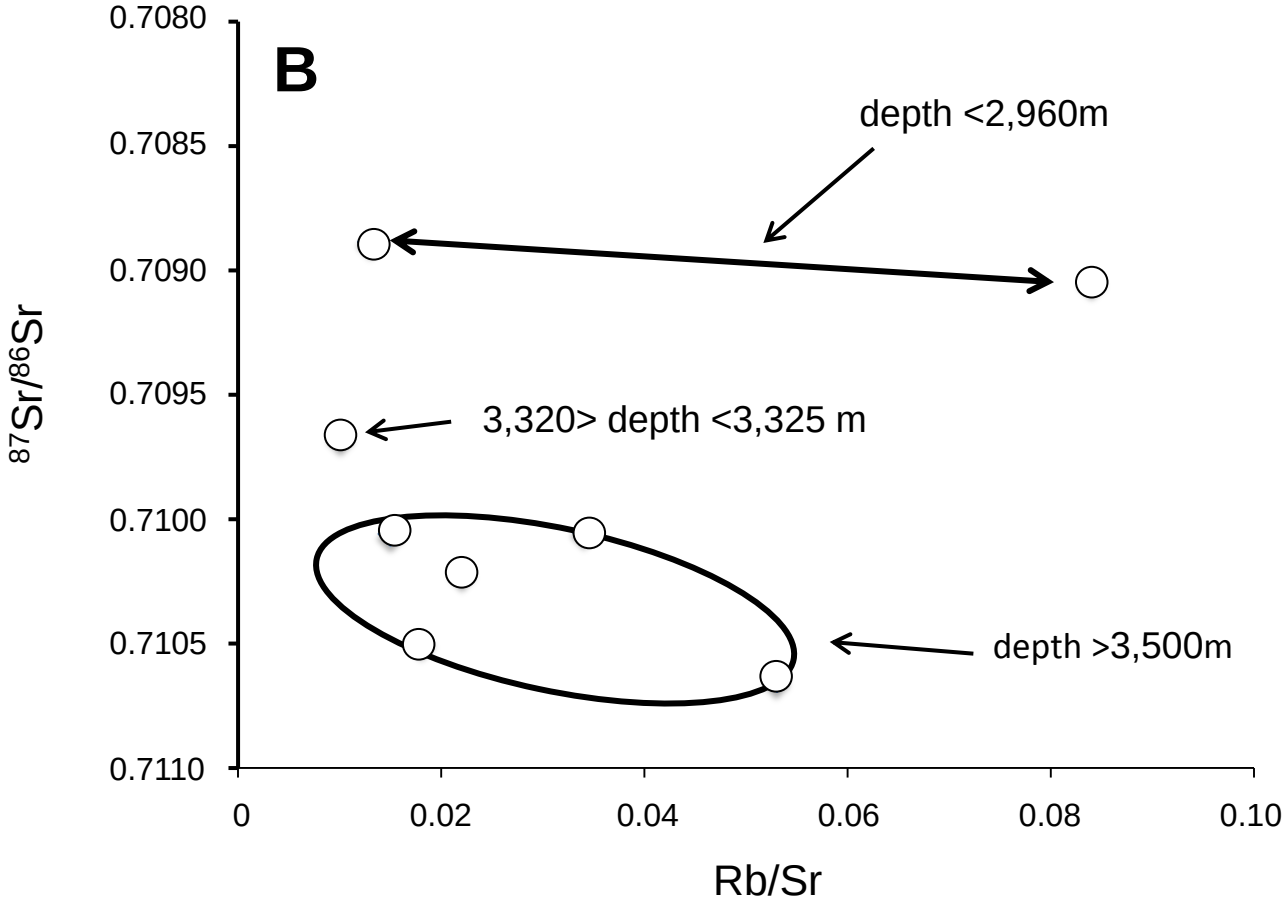
B
0.7080
0.7085
0.7090
0.7095
0.7100
0.7105
0.7110
$^{87}Sr/^{86}Sr$
depth <2,960m
3,320> depth <3,325 m
depth >3,500m
0
0.02
0.04
0.06
0.08
0.10
Rb/Sr

Sample ID	Si (ng/g)	Al (ng/g)	Mg (ng/g)	Ca (ng/g)	Fe (ng/g)	Mn (ng/g)	Rb (ng/g)	Sr (ng/g)	Rb/Sr	Ca/Sr	$^{87}Sr/^{86}Sr$ (+/- 2σ)
NW Peciko-3											
C1-2730.3	0.39	179	22.3	124	0.02	2.39	6.29	387	0.016	0.320	0.708743 (16)
C1-2737.2	0.41	29.3	40.1	74.0	0.05	4.11	5.43	454	0.012	0.163	0.708794 (16)
C1-2747.0	0.88	266	2.64	7.03	0.63	bdl	2.19	56.2	0.039	0.125	-
C2-2764.5	0.46	4.9	109	189	0.02	0.47	3.80	1322	0.003	0.143	0.708830 (22)
C2-2766.1	-	-	-	-	-	-	-	-	-	-	0.708975 (16)
C2-2768.1	1.04	243	59.5	214	23.6	9.61	4.46	271	0.016	0.790	0.708524 (18)
C2-2778.7	0.80	936	75.4	169	2.83	4.89	6.80	417	0.016	0.405	0.708711 (46)
C2-2779.2	1.26	977	38.8	105	3.61	3.32	10.2	217	0.047	0.484	0.708941 (18)
C3-3116.9	0.89	1111	59.1	93.4	8.85	bdl	5.11	1021	0.005	0.091	0.709422 (18)
C3-3117.9	0.87	143	32.2	90.7	1.46	0.56	4.20	500	0.008	0.181	0.709369 (20)
C4-3131.4	1.06	51.0	47.1	108	0.67	0.36	4.26	528	0.008	0.205	0.709338 (16)
C4-3140.9	0.82	287	73.9	167	1.76	12.2	6.98	1061	0.006	0.157	0.709228 (16)
C4-3145.0	0.51	21.4	64.7	156	0.06	0.99	2.53	536	0.005	0.291	0.709271 (16)
C5-3176.2	0.52	605	32.6	95.3	9.35	1.64	2.56	344	0.007	0.244	0.709359 (16)
C5-3177.3	0.45	74.8	25.5	69.9	0.79	1.19	1.60	286	0.006	0.244	0.709285 (14)
C7-3381.0	0.42	363	71.7	108	0.07	8.51	3.01	242	0.012	0.446	0.709659 (14)
C7-3383.5	0.77	7.1	41.1	76.5	0.02	0.21	3.22	348	0.009	0.220	-
C7-3384.5	0.42	13.5	26.9	46.0	0.23	0.07	2.45	242	0.010	0.187	0.709384 (14)
C7-3386.2	0.66	27.3	29.8	83.5	0.19	0.30	3.18	334	0.010	0.250	0.710053 (18)
C8-3517.4	0.58	3.40	45.2	111	4.74	1.43	1.87	143	0.013	0.776	0.709872 (18)
C9-3540.5	0.86	3.30	26.4	108	1.34	0.44	2.61	284	0.009	0.380	0.709956 (16)
C9-3553.0	0.56	9.79	25.6	72.0	0.20	0.14	3.33	329	0.010	0.219	0.710259 (20)
C9-3556.6	0.44	15.6	14.6	33.1	0.04	0.04	2.89	205	0.014	0.161	0.710327 (16)
NW Peciko-8											
C1-2932.6	1.66	311	43.6	152	6.90	3.61	10.8	129	0.084	1.178	0.709048 (22)
C2-2959.4	0.41	13.0	208	242	0.04	18.0	4.33	325	0.013	0.745	0.708884 (18)
C3-3320.4	0.78	27.0	35.9	85.5	0.01	0.24	3.19	310	0.010	0.276	0.709671 (16)
C3-3322.4	0.70	19.1	86.8	165	0.02	6.64	-	-	-	-	0.709577 (16)
C5-3505.8	0.61	74.6	16.4	52.3	0.17	0.41	3.22	149	0.022	0.351	0.710219 (18)
C5-3515.7	0.96	107	75.1	127	51.5	9.00	1.95	128	0.015	0.992	0.710059 (20)
C6-3534.4	0.62	21.2	7.51	12.5	0.08	0.07	4.19	79.3	0.053	0.158	0.710646 (16)
C6-3536.4	0.44	24.0	27.6	49.1	0.12	0.71	5.35	158	0.034	0.311	0.710048 (16)
C6-3538.3	0.74	20.0	32.8	68.0	0.08	0.29	4.36	238	0.018	0.286	0.710495 (18)

contents are in ppb

Sample ID	Cr (ng/g)	Co (ng/g)	Ni (ng/g)	Cu (ng/g)	Zn (ng/g)	Br (ng/g)	Ba (ng/g)	Cs (ng/g)	Sn (ng/g)
NW Peciko 3									
C1-2730.3	8.82	30.3	2.50	11.6	79.9	482	87.6	0.11	bdl
C1-2737.2	3.78	2.62	2.50	5.20	0.38	167	37.6	0.06	0.003
C1-2747.0	12.9	3.10	8.89	9.63	2.02	91.2	47.8	0.06	0.022
C2-2764.5	9.25	7.31	9.17	7.42	1.85	548	26.3	0.08	0.006
C2-2768.1	38.6	637	923	442	2099	661	29.6	0.12	0.025
C2-2778.7	12.0	104	185	24.7	201	196	15.2	0.07	bdl
C2-2779.2	11.7	474	721	155	1627	339	18.3	0.12	bdl
C3-3116.9	18.3	12.7	37.1	32.6	8.26	158	28.2	0.09	0.04
C3-3117.9	13.3	12.8	30.2	30.0	5.35	67.8	29.9	0.06	bdl
C4-3131.4	28.5	5.99	7.25	7.24	6.67	175.4	25.8	0.08	bdl
C4-3140.9	32.9	93.3	136	12.2	83.0	90.5	13.6	0.14	0.017
C4-3145.0	12.1	7.42	15.5	4.89	9.32	108	16.2	0.05	0.023
C5-3176.2	15.3	13.3	28.8	9.76	12.0	73.5	25.4	0.03	bdl
C5-3177.3	13.8	12.6	11.9	5.86	13.2	80.1	22.2	0.03	bdl
C7-3381.0	13.2	145	252	3.24	169	49.2	10.2	0.06	bdl
C7-3383.5	13.1	3.20	2.27	5.15	2.85	56.0	21.0	0.04	bdl
C7-3384.5	17.6	2.34	1.11	4.14	1.89	65.9	30.2	0.04	bdl
C7-3386.2	16.9	3.14	5.40	5.56	5.08	82.8	21.7	0.05	bdl
C8-3517.4	14.4	14.2	166	2.63	44.6	13.7	14.8	0.06	bdl
C9-3540.5	12.3	6.19	5.83	3.74	16.4	154	35.0	0.06	bdl
C9-3553.0	13.7	3.00	3.15	6.09	2.24	151	18.3	0.07	bdl
C9-3556.6	13.6	2.68	bdl	6.97	1.10	106	20.8	0.04	bdl
NW Peciko 8									
C1-2932.6	22.8	764	1356	398	1529	87.9	15.5	0.30	0.007
C2-2959.4	13.0	58.0	143	7.55	13.5	67.6	9.35	0.08	bdl
C3-3320.4	13.8	1.71	0.09	5.83	5.74	29.1	18.7	0.05	bdl
C3-3322.4	27.8	32.2	46.2	4.68	85.6	44.3	14.5	0.09	0.07
C5-3505.8	10.6	8.18	13.2	25.2	12.3	13.3	29.3	0.07	bdl
C5-3515.7	6.95	492	767	112	504	17.5	11.7	0.06	bdl
C6-3534.4	16.8	4.78	9.48	29.8	4.42	35.1	32.0	0.06	bdl
C6-3536.4	12.9	25.6	38.9	16.5	43.3	21.2	25.6	0.10	bdl
C6-3538.3	14.8	2.08	bdl	2.48	4.53	33.2	19.1	0.08	bdl

bdl stands for below detection limit

Sample #	La (ng/g)	Ce (ng/g)	Pr (ng/g)	Nd (ng/g)	Sm (ng/g)	Eu (ng/g)	Gd (ng/g)	Tb (ng/g)	Dy (ng/g)	Ho (ng/g)	Er (ng/g)	Tm (ng/g)	Yb (ng/g)	Lu (ng/g)	Σ REEs (ng/g)	La/Yb
NW Peciko-3																
C1-2730.3	0.02	0.11	0.02	0.25	0.17	0.02	0.12	0.02	0.11	0.01	0.03	bdl	0.05	bdl	0.93	0.40
C1-2737.2	0.01	bdl	bdl	0.006	0.05	0.01	0.01	0.006	0.01	0.004	0.007	bdl	0.02	bdl	0.13	0.50
C1-2747.0	0.02	0.13	0.03	0.13	0.04	0.002	0.03	0.01	0.06	0.01	0.05	0.002	0.03	bdl	0.54	0.67
C2-2764.5	bdl	0.003	0.002	0.07	0.03	bdl	0.03	0.005	0.009	0.005	0.02	bdl	0.04	0.003	0.20	-
C2-2768.1	11.2	61.5	12.1	87.6	38.7	12.0	49.9	7.57	36.7	6.06	13.8	1.58	8.78	1.11	349	1.28
C2-2778.7	0.91	5.10	0.99	6.85	2.64	0.84	4.12	0.64	2.91	0.45	1.00	0.11	0.47	0.06	27.1	1.94
C2-2779.2	3.49	21.3	3.76	24.4	12.2	4.22	18.5	3.23	14.8	2.11	5.00	0.50	2.75	0.31	117	1.27
C3-3116.9	0.24	1.12	0.17	1.01	0.58	0.18	0.75	0.14	0.91	0.18	0.50	0.09	0.29	0.06	6.16	0.83
C3-3117.9	0.05	0.31	0.04	0.26	0.13	0.04	0.15	0.04	0.26	0.04	0.10	0.01	0.13	0.01	1.57	0.38
C4-3131.4	0.04	0.14	0.02	0.15	0.07	0.01	0.08	0.02	0.09	0.02	0.01	0.02	0.04	0.01	0.72	1.00
C4-3140.9	0.86	2.72	0.35	2.20	0.65	0.21	0.97	0.18	0.88	0.17	0.33	0.04	0.27	0.03	9.86	2.17
C4-3145.0	0.07	0.31	0.03	0.28	0.10	0.01	0.10	0.03	0.07	0.02	0.03	0.004	0.08	0.007	1.41	0.88
C5-3176.2	0.24	0.89	0.15	0.70	0.31	0.10	0.35	0.10	0.52	0.10	0.37	0.03	0.31	0.05	4.22	0.77
C5-3177.3	0.04	0.17	0.03	0.25	0.08	0.03	0.18	0.03	0.21	0.04	0.16	0.02	0.14	0.01	1.37	0.29
C7-3381.0	0.66	2.36	0.42	2.39	0.80	0.25	1.48	0.18	0.93	0.22	0.39	0.03	0.20	0.03	10.3	3.30
C7-3383.5	0.01	0.03	0.01	0.03	0.03	bdl	0.01	0.02	0.04	0.01	0.03	0.004	0.03	bdl	0.25	0.33
C7-3384.5	0.01	0.04	bdl	0.05	0.02	bdl	0.06	0.004	0.05	0.005	0.03	0.004	0.05	bdl	0.32	0.20
C7-3386.2	bdl	0.05	0.02	0.13	0.04	0.07	0.05	0.01	0.08	0.01	0.01	0.001	0.03	0.001	0.50	-
C8-3517.4	0.02	0.04	0.01	0.06	0.04	bdl	0.07	0.02	0.06	0.02	0.03	0.01	0.04	bdl	0.42	0.50
C9-3540.5	0.03	0.07	0.01	0.09	0.05	0.03	0.06	0.02	0.03	0.02	0.02	0.01	0.04	0.001	0.46	0.75
C9-3553.0	0.005	0.02	0.009	0.05	0.10	0.008	0.04	0.01	0.02	0.007	0.03	0.007	0.03	bdl	0.34	0.17
C9-3556.6	0.005	0.02	0.001	0.08	0.04	bdl	0.06	0.01	0.02	0.01	0.01	bdl	0.06	0.001	0.31	0.08
NW Peciko-8																
C1-2932.6	3.92	32.7	9.26	87.8	46.6	16.1	65.9	10.7	49.8	7.98	17.0	1.73	8.50	1.07	359	0.46
C2-2959.4	0.006	0.004	0.016	0.04	0.07	bdl	0.04	0.004	0.05	0.02	0.02	0.006	bdl	bdl	0.28	-
C3-3320.4	bdl	bdl	0.005	0.03	0.07	bdl	0.03	0.008	0.02	0.01	0.01	bdl	0.02	bdl	0.20	-
C3-3322.4	bdl	0.03	bdl	0.05	bdl	0.002	0.02	bdl	0.02	0.006	0.003	bdl	bdl	0.007	0.14	-
C5-3505.8	0.08	0.06	0.004	0.10	0.06	0.04	0.10	0.02	0.07	0.02	0.05	0.008	0.06	0.004	0.68	1.33
C5-3515.7	2.64	21.7	5.08	39.0	17.2	6.03	23.2	3.38	15.5	2.34	4.88	0.49	2.39	0.30	144	1.10
C6-3534.4	bdl	0.03	0.08	0.06	0.10	0.008	0.06	0.01	0.04	0.01	0.02	0.001	0.02	0.003	0.44	-
C6-3536.4	0.02	0.10	0.03	0.18	0.07	0.02	0.17	0.02	0.17	0.03	0.02	0.01	0.05	0.001	0.89	0.40
C6-3538.3	bdl	bdl	0.008	0.02	0.06	0.005	0.05	0.008	0.07	0.007	0.03	0.001	0.03	0.001	0.29	-

bdl stands for below detection limit

Sample IDs	$^{87}Sr/^{86}Sr$ (± 2σ) H_2O leachates	$^{87}Sr/^{86}Sr$ (± 2σ) HCl leachates	$^{87}Sr/^{86}Sr$ H_2O/HCl
NW Peciko-3			
C1-2737.2	0.708794 (16)	0.708551 (18)	>0.000243
C1-2747.0	-	0.708606 (18)	-
C2-2764.5	0.708830 (22)	0.708573 (16)	>0.000257
C2-2766.1	0.708975 (16)	0.708946 (16)	>0.000029
C2-2768.1	0.708524 (18)	0.708660 (18)	<0.000136
C2-2778.7	0.708711 (46)	0.708617 (50)	>0.000094
C2-2779.2	0.708941 (18)	0.708817 (20)	>0.000124
C3-3116.9	0.709422 (18)	0.709237 (18)	>0.000185
C3-3117.9	0.709369 (20)	0.708668 (14)	>0.000132
C4-3131.4	0.709338 (16)	0.709112 (18)	>0.000226
C4-3140.9	0.709228 (16)	0.709074 (18)	>0.000154
C4-3145.0	0.709271 (16)	0.709150 (18)	>0.000121
C5-3176.2	0.709359 (16)	0.709103 (18)	>0.000256
C5-3177.3	0.709285 (14)	0.709173 (18)	>0.000112
C7-3381.0	0.709659 (14)	0.709409 (18)	>0.000255
C7-3383.5	-	0.708808 (16)	-
C7-3384.5	0.709384 (14)	0.709200 (14)	>0.000184
C7-3386.2	0.710053 (18)	0.709551 (16)	>0.000502
C8-3517.4	0.709872 (18)	0.709321 (16)	>0.000551
C9-3540.5	0.709956 (16)	0.709226 (14)	>0.000730
C9-3553.0	0.710259 (20)	0.709554 (18)	>0.000705
C9-3556.6	0.710327 (16)	0.709610 (16)	>0.000717
NW Peciko-8			
C1-2932.6	0.709048 (22)	0.708935 (14)	>0.000113
C2-2959.4	0.708884 (18)	0.708811 (16)	>0.000073
C3-3320.4	0.709671 (16)	0.709242 (16)	>0.000229
C3-3322.4	0.709577 (16)	0.709260 (52)	>0.000317
C5-3505.8	0.710219 (18)	0.709062 (16)	>0.000657
C5-3515.7	0.710059 (20)	0.709818 (22)	>0.000241
C6-3534.4	0.710646 (16)	0.710110 (18)	>0.000536
C6-3536.4	0.710048 (16)	0.709824 (16)	>0.000224
C6-3538.3	0.710495 (18)	0.709514 (16)	>0.000981